

# Crewed Mission to Callisto Using Advanced Plasma Propulsion Systems

R.B. Adams<sup>\*1</sup>, G. Statham<sup>†1,2</sup>, S. White<sup>1,2</sup>, B. Patton<sup>3</sup>, Y.C.F. Thio<sup>4</sup>, R. Alexander<sup>1</sup>, S. Fincher<sup>1</sup>, T. Polsgrove<sup>\*1</sup>, J. Chapman<sup>1</sup>, R. Hopkins<sup>1</sup> and A. Philips<sup>1</sup>

<sup>1</sup> NASA Marshall Space Flight Center, Advanced Concepts Department, Huntsville, AL 35812, USA.

<sup>2</sup> ERC Inc., 555 Sparkman Drive, Executive Plaza, Suite 1622, Huntsville, AL 35816, USA

<sup>3</sup> NASA Marshall Space Flight Center, Propulsion Research Center, Huntsville, AL 35812, USA.

<sup>4</sup> U.S. Department of Energy, Office of Fusion Energy Sciences, 19901 Germantown Road, Germantown, MD 20874

<sup>5</sup> Institute of Fusion Technology, University of Wisconsin, Madison, WI 20874, USA

**Abstract.** This paper describes the engineering of several vehicles designed for a crewed mission to the Jovian satellite Callisto. Each subsystem is discussed in detail. Mission and trajectory analysis for each mission concept is described. Crew support components are also described. Vehicles were developed using both fission powered magneto plasma dynamic (MPD) thrusters and magnetized target fusion (MTF) propulsion systems. Conclusions were drawn regarding the usefulness of these propulsion systems for crewed exploration of the outer solar system.

## INTRODUCTION

Administrator Daniel Goldin initiated the Revolutionary Aerospace Systems Concepts (RASC) activity starting in fiscal year 2001 to address conceptual design of systems and architectures for potential missions 25 to 40 years in the future. The results of these designs were to determine the technologies and infrastructure necessary to enable those missions. Consequently RASC studies were intended to take a “top-down” approach.

In fiscal year 2002 RASC organized the Human Outer Planet Exploration (HOPE) group to investigate the possibility of crewed travel to the outer solar system. Three scenarios were considered, nuclear thermal propulsion using crewed and support vehicles, nuclear electric propulsion also using crewed and support vehicles and fusion propulsion using crewed vehicles only. The outer solar system from the asteroid belt and beyond was surveyed to select a suitable baseline destination point. Using assumptions on requirements and available technology three centers (GRC, LaRC and MSFC) designed vehicles to support a crewed trip to the outer solar system. The emphasis on this study was to gain a greater understanding of the challenges associated with these missions so that they can be addressed now. This paper outlines the mission analysis and vehicle designs developed from the MSFC led contribution to this project. The detailed design of one of the engine concepts, Magnetized Target Fusion, is outlined in another paper at this conference<sup>1</sup>. Additionally the full results from this study were documented by the authors in a NASA Technical Paper<sup>2</sup>.

## SELECTED DESTINATION

A number of candidate destinations were considered before the final selection was made. The major selection criteria can be summarized as follows. The destination should be a body in the outer solar system, here defined as being beyond the orbit of Mars, it should be suitable for human surface exploration and it should contain

---

\* AIAA Member

† AIAA Senior Member

some features of legitimate scientific interest. The requirement for human surface exploration ruled out any of the gas giant planets, Jupiter, Saturn, Uranus and Neptune, but not their extensive satellite systems. As a final criterion, one that was effectively internal to the HOPE program, it was desirable that the destination present a suitable level of challenge to the design team.

Amongst the short-listed candidates were the following bodies:

- Ceres; the largest asteroid, with a diameter of almost 1000 km, located in the main belt. Scientific interest is largely focused on determining the composition and structure of the asteroids as a key to understanding the formation and development of the Solar System. Asteroidal mining and planetary defense considerations prompt additional interest. Due to its relatively close proximity and low mass, Ceres presents a simpler set of design challenges than more distant destinations.
- Europa; the smallest of Jupiter's Galilean satellites and the second closest to the planet itself. Scientific interest is largely prompted by the likely presence of a submerged ocean with tidal-heating, which could offer conditions conducive to the development of life. Europa's location, within the Jovian radiation belts, poses significant design problems, particularly when contemplating human surface exploration.
- Callisto; the second-largest Galilean satellite and the most distant from Jupiter itself. Scientific interest is prompted by the possibility of subsurface water. Callisto's distance from Jupiter places it in a significantly less hazardous radiation environment than Europa, potentially permitting human surface operations.
- Titan; the largest satellite of Saturn and one of the largest in the Solar System. Scientific interest is considerable, in part because Titan appears to be more complex than other satellites, with a significant (and opaque) atmosphere, possibly offering conditions conducive to the development of life. The relative remoteness of Saturn is offset by the absence of any significant radiation belts.
- Chiron; an unusual minor planet, following an eccentric orbit with perihelion just outside the orbit of Saturn and aphelion just within that of Uranus. Scientific curiosity is prompted by Chiron's visible coma and variable brightness, which appears to indicate that volatile compounds are being vaporized from this, in other respects, asteroidal body. It is hypothesized that Chiron has only occupied its present orbit for a relatively short period, having previously been located in the (trans-Neptunian) Kuiper Belt. Access to Chiron could yield important data about the composition and structure of Kuiper Belt objects that are thought likely to be remnant objects from the Solar System's formation. Its remoteness and low temperature would pose significant technical problems.
- Triton; the largest satellite of Neptune and the only significant satellite in the Solar System that follows a retrograde orbit. Scientific interest is due to its continuing seismic activity, as manifested by several "ice" volcanoes, and the likelihood that Triton is a Kuiper Belt object, captured by Neptune in the relatively recent past. Triton's remoteness and low temperature pose significant design challenges.

The Jovian moon Callisto was selected because of the balance which it offers between scientific interest, design challenge severity and the level of hazard to human operations posed by the local environment.

## VEHICLE DESIGN

MSFC's original task was to consider only nuclear fusion propulsion techniques for the HOPE mission. The initial techniques selected for study were: the Spherical Torus concept, developed by Williams et al.<sup>3</sup>; the Magnetized Target Fusion (MTF) concept, developed by Thio et al.<sup>4</sup>; and the VISTA concept, developed by Orth et al.<sup>5</sup> These three concepts cover the range of fusion techniques, from continuous magnetic confinement to pulsed inertial confinement. Fusion concepts employing antimatter were not considered as their level of development seemed too low to support a vehicle conceptual design.

One of the major ground rules for this study was that the crew could only be exposed to microgravity for a cumulative total time of one year. In this context, microgravity was defined as being any acceleration less than

one eighth of standard Earth gravity. None of the candidate propulsion systems is capable of accelerating the vehicle sufficiently to provide this level of apparent gravity, so any missions lasting longer than a year would automatically require a separate artificial gravity system. All of the fusion-propelled concepts were developed using a total mission time of one year and a crew stay time on the target planet of one month. As the surface gravity on Callisto is one eighth of a standard Earth gravity, time spent on the surface did not contribute towards the one-year microgravity total. All of the concepts above are capable of performing such a mission, but in some cases, the initial vehicle mass was extremely high.

Unfortunately, although there is an excellent and well-documented design study on the Spherical Torus concept available in the literature<sup>3</sup>, information on scaling the device is not readily obtainable. For the VISTA concept, information in the literature is less abundant and once again, there is no scaling data. The lack of scaling data for these two concepts meant that the MSFC design team had to use the point designs taken directly from in the literature, without any adjustments, in order to complete preliminary vehicle designs to the selected destination. Unfortunately, the resulting vehicle designs were non-competitive, in part due to the fact that the engine designs used had been optimized for somewhat different missions. As a result, MTF emerged from this preliminary process as the most promising propulsion concept.

Several different options for MTF were considered. A MTF system based on the D-D reaction was adopted as the baseline, but an alternate system, based on the D-He3 reaction, was also retained as an advanced option. The fission concepts developed by the other centers required a 180-day crew time on Callisto. The stay time was defined by the need to wait for Jupiter and Earth to come back into optimum alignment and reduce the total vehicle  $\Delta V$  requirement. The HOPE study lead therefore requested that the MSFC team consider a fusion option with a 180-day stay time so as to facilitate comparison with results produced by the other (non-fusion) teams. A parametric analysis of total mission time showed that a time of 1 $\frac{3}{4}$  years substantially reduced mission  $\Delta V$  requirements. A one-year mission required the vehicle to fly retrograde on both outbound and inbound legs. In contrast, the 1 $\frac{3}{4}$  yr mission avoided this problem and, although nearly doubling trip time, reduced the acceleration requirements. Of course the longer trip time necessitated incorporation of an artificial gravity system into the vehicle design, but the associated mass penalty was minor compared to the gains achieved.

From this wide range of cases, three MTF options were selected for presentation: MTF D-D 30 day stay; MTF D-D 180 day stay; and MTF D-He3 180 day stay.

Near the end of the study, MSFC also conducted some analysis of non-fusion propelled vehicle concepts. Several technologies that appear to increase performance of the nuclear-fission electric propulsion options were considered. The baseline nuclear electric option for these studies was a solid core NERVA-style reactor with a Brayton power conversion system and a magnetoplasmadynamic thruster assembly. MSFC investigated an alternate option in which the reactor and power conversion system was replaced by a molten salt reactor and liquid metal Rankine power conversion system. Additionally MSFC investigated a system that replaced the Brayton cycle with a magnetohydrodynamic power conversion system. Unlike the baseline MTF case, these concepts all required a five-year mission time and split mission profile (i.e. separate crew and cargo vehicles)..

## **Payload Components**

The payload components of the HOPE vehicles consist of a Trans-Hab module, a surface habitat, a lander, and an In-Situ Resource Utilization (ISRU) plant. These components are responsible for providing a habitable environment on the vehicle and on the surface of Callisto as well as supporting the exploration team as it collects scientific data. The Trans-Hab forms the main living quarters for the six-crew members. This module has a mass of approximately 40 metric tons and contains an additional 4 metric tons of consumables. An example of the Transhab concept is shown in Figure 1.

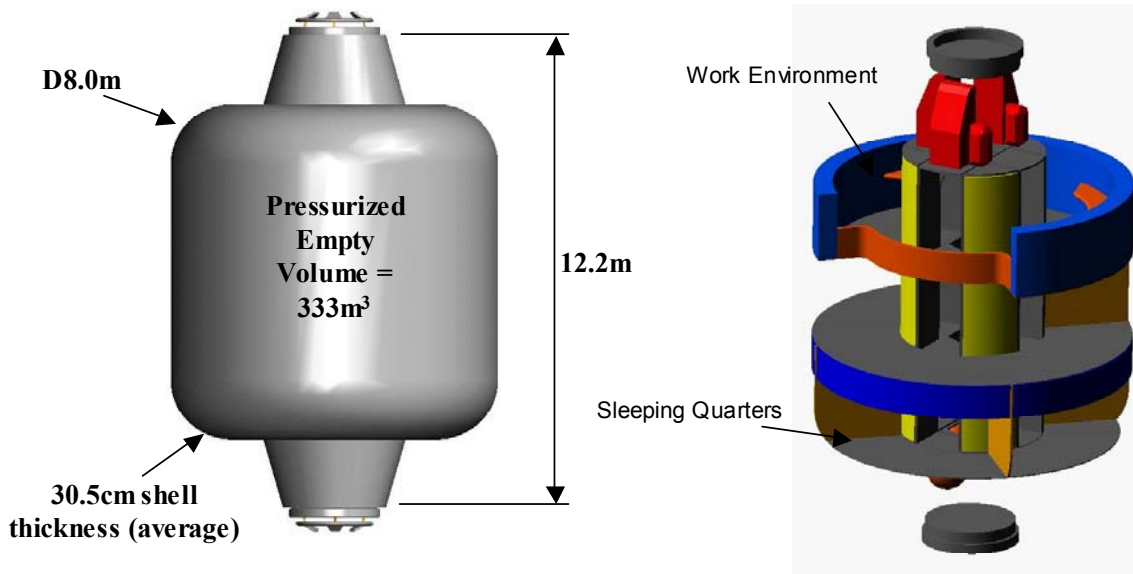


Figure 1 – Transhab configuration and layout<sup>6</sup>

The surface habitat is an inflatable structure that can house three crew members on the surface of Callisto. It is responsible for providing shelter to the surface crew and serves as a laboratory from which surface experiments are conducted. A 250-kilowatt electric (1 megawatt thermal) reactor, located 1 kilometer away, will generate power for transmission to the surface habitat. Figure 2 depicts the conceptual design of the surface habitat.

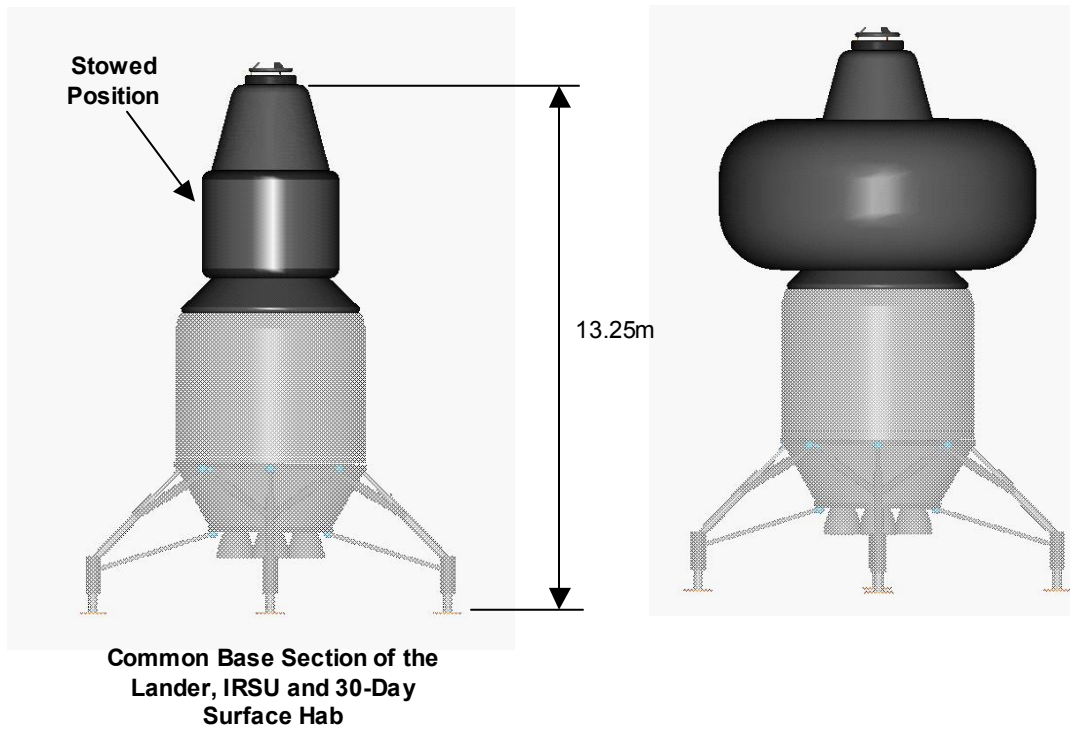


Figure 2 – Configuration of the surface habitat. Living area uses inflation technology similar to Transhab<sup>6</sup>

The lander is used to transport crew and materials between the surface of Callisto and the orbiter. It is capable of carrying up to 40 metric tons down to the surface. Its fuel is produced from resources present on the surface of Callisto. The lander is shown in Figure 3.

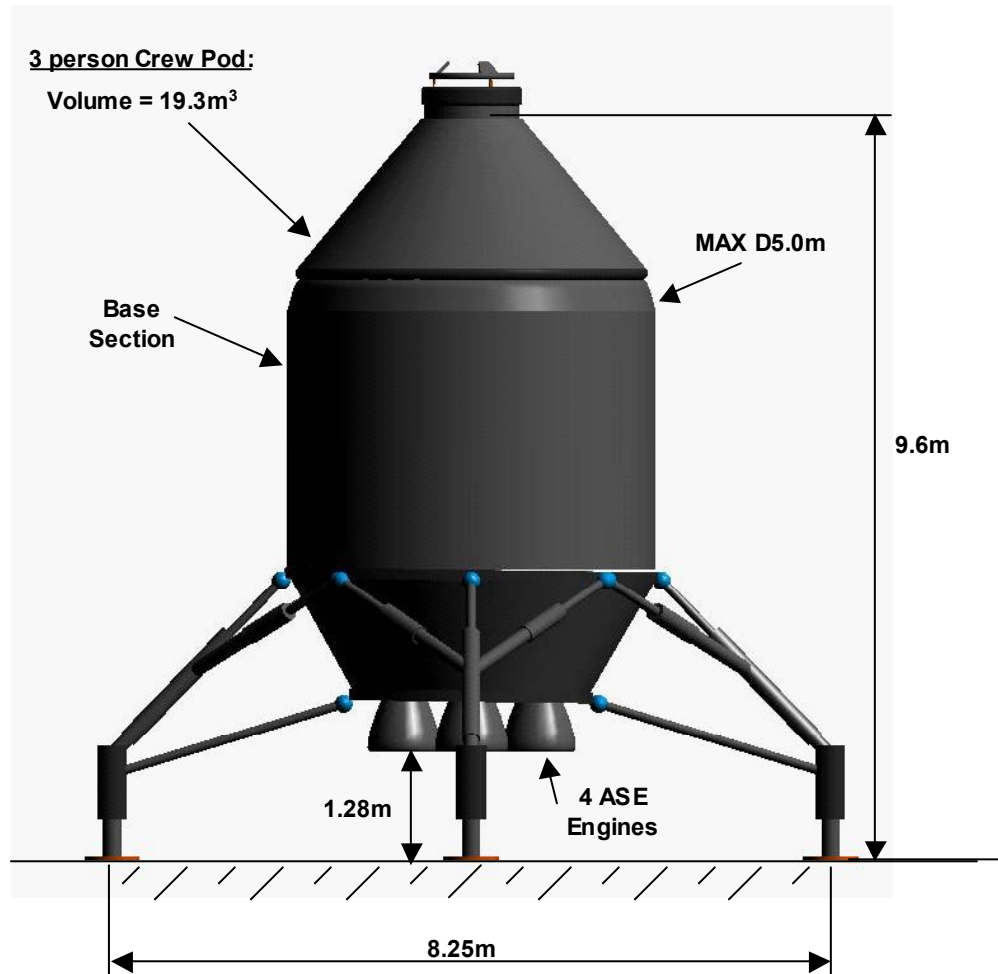
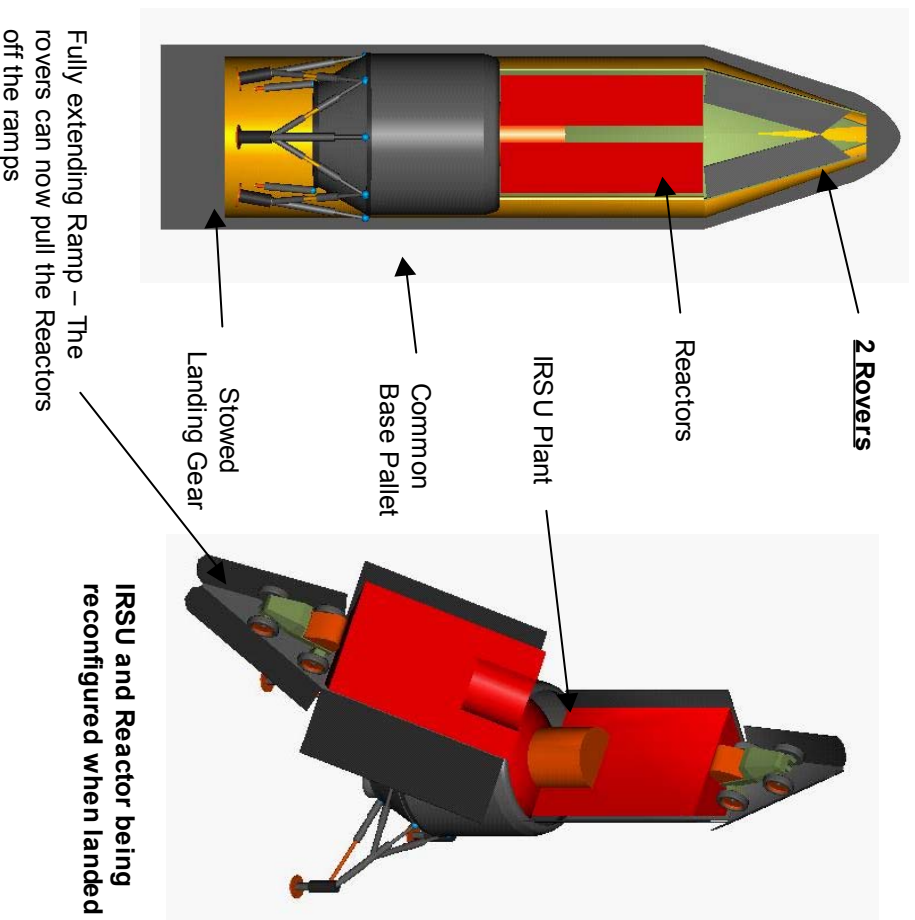


Figure 3 – Configuration of the crewed lander<sup>6</sup>

Callisto is a desolate satellite with a higher surface density of impact craters than any other object in the solar system. Its crust dates back 4 billion years; to around the time at which the solar system was formed. This ancient surface may be able to provide valuable information about the state of the early solar system. In addition to scientific information, Callisto will also be able to provide mission resources (e.g. propellant for the mission lander).

Callisto has a density of  $1.86 \text{ gm/cm}^3$ , and is comprised of ice and rock. The 200 km thick crust is an icy layer that could be mined for water. Beneath the crust is believed to be an ocean of salt and water, 10 km deep. Because Callisto contains such an abundance of water, it can provide a variety of resources. Through simple distillation and dissociation processes, oxygen and hydrogen can be produced for fuel and air. The In-Situ Resource Utilization (ISRU) unit will convert the icy regolith of Callisto into water, Liquid Oxygen (LOX) and liquid hydrogen at a rate equivalent to 21 kg of water per hour. This will provide enough propellant for the lander to rendezvous with the orbiter every thirty days. The ISRU will require a power of 215 kilowatts. Figure 4 illustrates the ISRU concept used in this study.



**Figure 4 – ISRU configuration and deployment. Reactors must be positioned away from the IRSU before commencement of operations.**<sup>6</sup>

One of the groundrules of the HOPE study is that all of the above systems, as well as any other payload launched from Earth, would fit inside an assumed launch vehicle fairing similar to that for a Delta IV Heavy. All of the vehicles described in this study can be broken down into their respective parts and launched within this fairing. Note that the fairing determined the size and shape of our propellant tanks. Some components, such as the MTF assembly, would require significant assembly on orbit after launching.

### **Reaction Control System**

The reaction control system (RCS) is based on an oxygen and hydrogen chemical propulsion system. Twenty-four 500-lbf thrusters are located in two ring frames on the vehicles structure and provide full six-degrees-of-freedom maneuvering capability for attitude control, docking and spin control for artificial gravity. During the outbound and inbound portions of the fight, the manned vehicle is spun at approximately one-and-a-quarter revolutions a minute to simulate 25% of Earth gravity. To accomplish both of these tasks up to 85,000 pounds of liquid oxygen and liquid hydrogen propellant are stored separately from the main drive propellant. These propellants are maintained in a liquid state by the liberal application of multi-layer insulation with any additional heat leakage into the system removed by cryo-coolers powered by the main electrical system. To ensure that the propellants are at the proper gaseous temperature and pressures required by these RCS thrusters, a series of run-tanks use electrical resistance heaters to convert the cryogenically stored liquid propellants into

the gaseous propellants required for the RCS thrusters. These run tanks are sized to hold approximately one meter per second  $\Delta V$  of gaseous propellant, which is available on-demand to the RCS thruster. If additional propellant is required beyond the one meter per second stored in the run tanks, the run tanks become a conditioning plenum, converting liquid cryogenic liquid propellant into gaseous propellant during high demand attitude control and artificial gravity spin maneuvers. In addition to the main RCS thrusters are a series of smaller 50 lbf hydrogen cold gas thrusters, which are used as needed for fine pointing and close proximity operations.

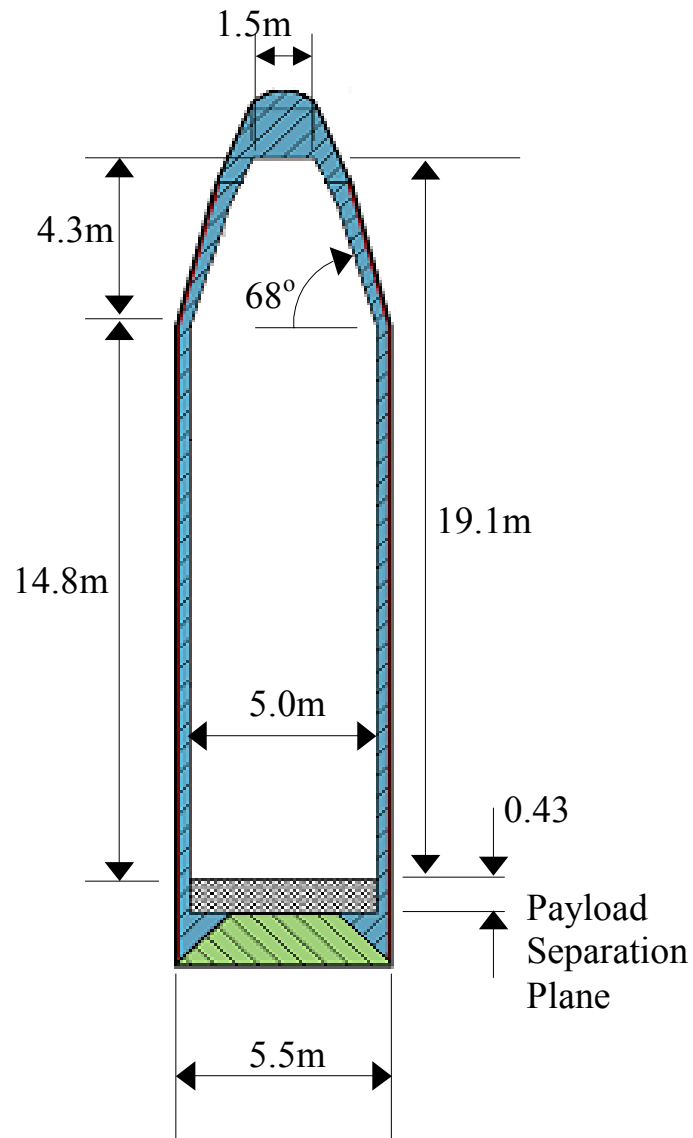
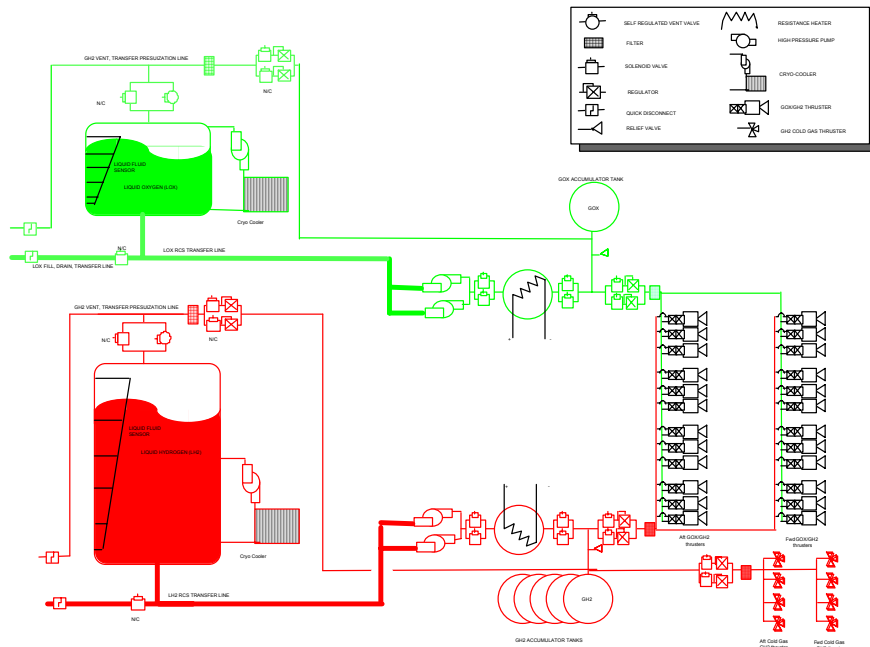


Figure 5 – Dimensions and configuration of expendable launch vehicle fairing assumed for this study.<sup>6</sup>



**Figure 6 – Gaseous Oxygen / Gaseous Hydrogen Reaction Control System with Liquid Propellant Storage**

### Structural Components

The main propellant tanks for this study were designed by the LVA (Launch Vehicle Analysis)<sup>7</sup> computer tool. The analysis was based on the assumption that the tanks were launched fully loaded with hydrogen. The tanks were not assumed to be pressure stabilized and no shroud was required. LVA analyzed the tanks using a full gamut of pre-launch, lift-off, and flight loads. The tanks have both fore and aft skirts that remain with them throughout the mission. The necessary docking equipment is launched within the skirts.

The main truss design was based on earlier manned Mars studies. With an on-orbit assembled truss, the designing loads are not the propulsion system thrust as is commonly thought. Most of the mass results from loads imparted during the ETO (Earth To Orbit) phase. Assembly and overall stiffness requirements are additional factors. Therefore, truss sections can serve different space missions with little or no change.

### Thermal Control Systems

There are three heat rejection systems for the HOPE vehicle: a low temperature radiator system for the avionics and crew, a medium temperature radiator for the power conversion system, and a high temperature radiator for the propulsion system waste heat. These radiators are necessary due to the need to maintain the systems within required temperature limits; in space, the only method of rejecting waste heat is through radiative heat transfer. All the radiator systems use heat pipes to distribute heat evenly across the panels. Figure 7 is a simplified schematic of the thermal control system for the power conversion system and the MTF engine.



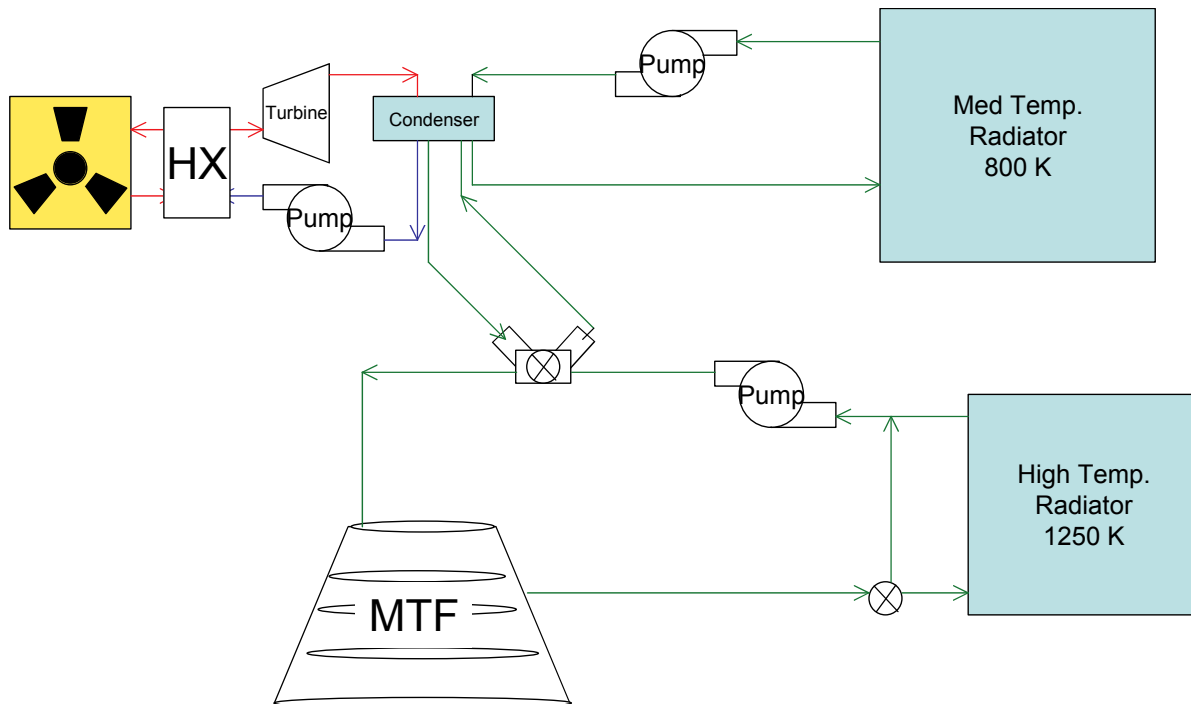


**Figure 7 - Schematic of Power Conversion and Engine Thermal Control Systems**

Thermal radiators for spacecraft systems need to be as lightweight as possible. However, some of the vehicle system requirements force the thermal radiator system to be heavier than would be necessary provided there was no other required functionality. The thermal radiator panels for advanced space vehicles of the type described in this document tend to have large surface areas, thus requiring that they be launched in a stowed configuration and deployed prior to usage. Deployment mechanisms add weight to the panel. Also, reliability and safety requirements will likely add weight to the system. Many analysts have attempted to analytically model these panels with various heat transport mechanisms and materials technology, to determine the weight of the system. Near term technology incorporates composite panels with heat pipes imbedded within the panels.

Eventually, for the system analysts, the input needed to model the radiator simplifies to a unit area or “areal density”. For advanced vehicles some analysts have estimated this unit weight be as low as  $1 \text{ kg/m}^2$  and as high as  $20 \text{ kg/m}^2$ . Of course, technology assumptions affect this number significantly. A more advanced technology assumption yields a lower unit weight. For HOPE the design team assumed near-to-mid term technology which led to the assumption that the high temperature radiator panels, with the deployment mechanisms, safety, and reliability, have a unit mass of  $10 \text{ kg/m}^2$  for single-sided or  $5 \text{ kg/m}^2$  for two-sided panels, while the medium temperature panels were assumed to weigh  $8 \text{ kg/m}^2$  ( $4 \text{ kg/m}^2$ ). The low temperature radiator panels have an assumed unit mass of  $3.7 \text{ kg/m}^2$  for two-sided panels. As a comparison, the International Space Station radiator panels weigh  $8.5 \text{ kg/m}^2$  for two-sided panels.

Analyses performed to size the radiator panels assumed that the panels have a perfect view to space with no view of the Sun. Also the infrared emissivity ( $\epsilon$ ) was assumed to be 0.9. Fin effectiveness was ignored and the panel was assumed to be at a constant average temperature. To calculate the radiator surface area the Stephan-Boltzmann equation is used. A radiator temperature was assumed, and based on the heat rejection requirements, a surface area was calculated with

$$q = \epsilon \sigma A_s T_s^4 \quad \text{Eq. 1}$$

The medium temperature radiator panels reject heat from the power conversion system at 800K. The panels employ a combination of water and sodium-potassium heat pipes. The higher temperature Na-K heat pipes are at the cooling fluid inlet to radiator with the water heat pipes near the cooler end. Figure 7 shows the radiator panel concept.

The heat rejection requirements vary with the concept being analyzed, and panel surface areas and masses vary accordingly. These are summarized below in Table 1.

**Table 1 - Medium Temperature Radiator Analysis Results Summary**

<i>Medium Temperature Radiator</i>			
<i>Concept</i>	D-D MTF 30 Day Stay	D-D MTF 180 Day Stay	D-He3 180 Day Stay
Heat Rejection Requirement (MW)	24.1	45.8	33.9
Heat Rejection Temperature (K)	800	800	800
Radiator Total Surface Area (m <sup>2</sup> )	1156.6	2192.3	1622.7
Radiator Mass (kg)	4614.5	10961.5	6490.9

The high temperature radiator panels reject the heat from the propulsion system. These panels use heat pipes with lithium as a working fluid. The temperature of these panels is assumed to be 1250K. The heat is collected in the propulsion system using a high temperature molten salt: FLiBe. The FLiBe passes through a heat exchanger to which the evaporator ends of the heat pipes are connected where it is cooled. The cooled fluid flows back in the engine completing the thermal control circuit. As with the medium temperature radiator the heat rejection requirements vary with the vehicle concepts and are summarized below in Table 2.

**Table 2 - High Temperature Radiator Analysis Results Summary**

<i>High Temperature Radiator</i>			
<i>Concept</i>	<i>D-D MTF 30 Day Stay</i>	<i>D-D MTF 180 Day Stay</i>	<i>D-He3 180 Day Stay</i>
Heat Rejection Requirement (MW)	261.9	497.9	176.5
Heat Rejection Temperature (K)	1250	1250	1250
Radiator Total Surface Area (m <sup>2</sup> )	2103.3	3998.6	1417.5
Radiator Mass (kg)	10516.5	19993	7087.3

Cryogenic refrigeration systems are used to maintain the LH<sub>2</sub> propellants during the transit to Callisto. Cryogenic hydrogen has a boiling point of about 20 K so that any heat leak into the tank affects the mission through propellant boil-off. For long-term missions, passive insulation systems are massive, accounting for the propellant boil-off during the mission. Zero boil-off (ZBO) systems use a combination of active and passive thermal control to provide a minimum mass solution. ZBO systems are comprised of : refrigerator, power system, controller, thermal radiator to reject the waste heat from the system and the insulation system that is comprised of multi-layer insulation and foam. The combination of the insulation and refrigeration system is optimized to attain the minimum system mass, taking into account the propellant selection.

The ZBO system sized for the HOPE mission uses present day cryo-cooler technology assuming 2-stage coolers for the LH<sub>2</sub> tanks. The mass and power calculations were based on research and analyses performed by NASA's Glenn Research Center, Marshall Space Flight Center and Ames Research Center. The analysis methodology takes into account the mass of the propellant, the size (surface area) of the propellant tanks, the

number of propellant tanks, and the type of propellant, tank pressure, and environmental conditions. Using this methodology a ZBO system can be adequately sized to maintain the required cryogenic propellant for the HOPE mission.

## Auxiliary Power

For the HOPE/RASC studies, a liquid metal potassium Rankine system was selected for the power conversion module for both the solid pin lithium cooled reactor (LMR) reactor and the Molten Salt reactor concepts.

Potassium Rankine systems are actually quite well characterized, as all of the major components (turbine, condenser, alternator and heat exchangers) have undergone many hours of extensive ground testing. One advantage of Rankine systems is that the heat is typically rejected at much higher temperatures (approximately 900 °K versus 425 °K for a Brayton cycle). Thus, the radiator mass tends to be much smaller for Rankine systems. This approximate “doubling” of the heat rejection temperature allows the radiator mass to be reduced approximately by a factor of 16, since  $2^4=16$ .

A schematic of a liquid metal Rankine conversion system is shown below in Figure 8.

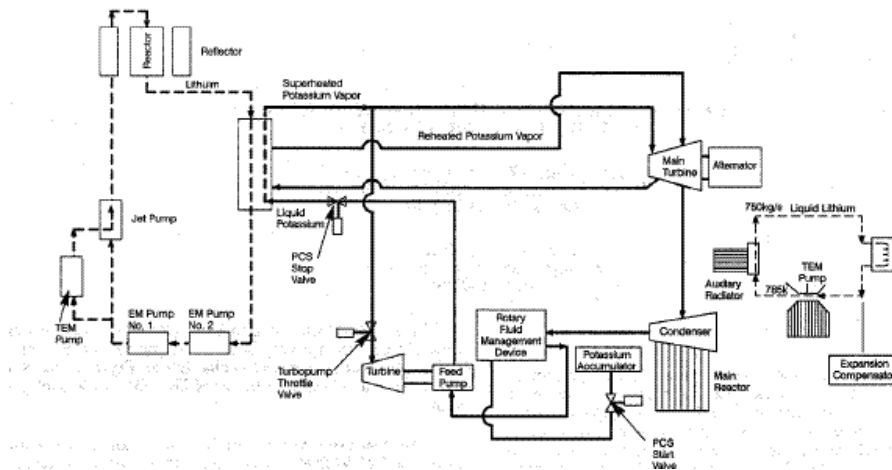


Figure 8 - Liquid metal Rankine conversion system<sup>8</sup>

A typical space system layout is shown in Figure 9. The liquid metal potassium Rankine cycle is similar to the typical steam cycle employed by the commercial utility industry, except that potassium is used as the working fluid.

The computer program ALKSYS was used for the APU design. The following discussion is taken directly from the ALKSYS users manual<sup>9</sup>.

“ In the power conversion system, the principal flow of dry, saturated potassium vapor leaving the boiler of the lithium-cooled reactor is diverted to the turbine of the turbo feed pump. As the vapor expands through the main turbine, inter-stage and external separators are used to maintain the liquid content of the stream at < 12% to avoid the potential for erosion of the turbine blades. Upon exhausting from the turbine, the vapor is condensed in tapered annular spaces surrounding the evaporator sections of the radiator heat pipes. Condensate is drawn from the small ends of the condensing annuli by a jet pump that is driven by a small stream of liquid taken from the discharge of

the turbine driven feed pump. Liquid discharging from the jet pump flows to the intake of the feed pump and is then pumped through the shell sides of a specified number of feed heaters (0 – 3) back to the boiler. One of the heaters is heated by feed pump turbine exhaust; other heaters, if more than one are specified, are heated by vapor extracted from appropriate stages in the main turbine or taken from the boiler outlet line if necessary, to provide the specified boiler feed temperature.

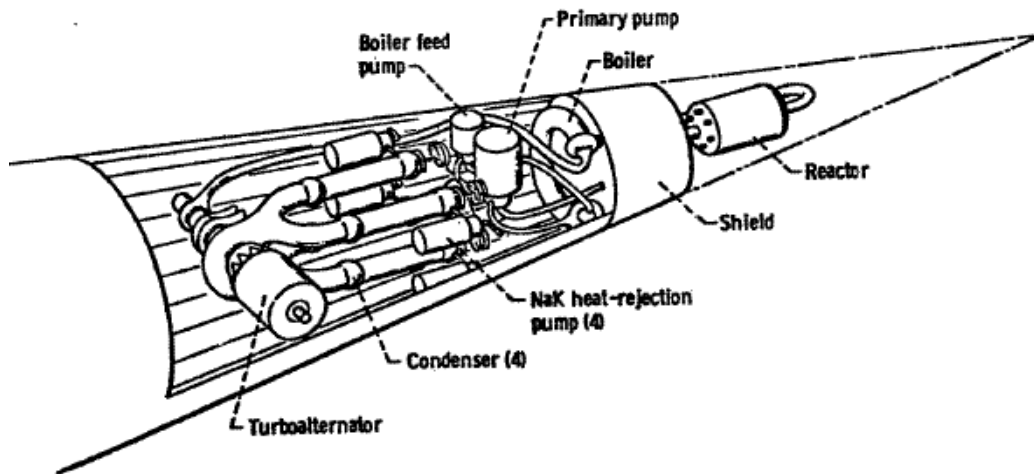


Figure 9 - Liquid metal Rankine system NEP vehicle layout<sup>10</sup>

Turbine blade tip velocity is a parameter that is dependent upon the strength of the turbine rotor material and is treated as an input variable in the model to allow evaluation of the effects of advanced rotor materials. This parameter has a strong effect on turbine size and rotational speed, and therefore, on the mass of the turbine and the generator.

Most of the required input information for the ALKSYS code operation pertains to the power conversion sub-model. Input includes turbine inlet and outlet temperatures, dry stage efficiency for the turbine, and the number of stages of feed heating.

The code outputs a complete mass and energy balance for the power conversion subsystem, as well as mass estimates for the major components.

The major heat rejection load from the power system is from the power turbine condenser. The heat is rejected by a heat pipe radiator operating at a temperature somewhat lower than that of the condenser. A smaller heat rejection load from cooling of the reactor shield and the turbine generator, is rejected by a low temperature heat pipe radiator.

The geometry of the radiators depends upon the power system rating. Input requirements for the heat rejection sub-model include launch vehicle bay dimensions and the operating temperature of the low

temperature radiator. Thermal loads for both parts of the radiator are provided by the power conversion sub-model, which provides dimensional information and the estimated mass of the heat rejection system.

The solid core reactor design is based on a fast spectrum, metallic-clad rod fuel element containing UN pellets. The primary coolant is lithium, hence it is similar to the SP-100 genre. The ALKYS code limits the peak pellet burn-up to 10 at % and the peak heat flux to 80 W/cm<sup>2</sup>. Rod diameter is determined by heat flux and burnup, but it is limited to 0.64 cm for mechanical stability. Reactor control is provided by in-core assemblies and by rotatable drums located around the core periphery. ASTAR-811C is used for the fuel rod cladding and structural components operating at temperatures above 1100 K, and Nb-1% Zr is used at lower temperatures. The design stress is two thirds of that which produces 1% creep during the system lifetime.

Two options are available in the ALKSYS code for estimating shield size and mass. In the two-pi option, the shield configuration and dimensions are selected to provide a fast neutron fluence of 10<sup>13</sup> neutrons/cm<sup>2</sup> and a total gamma dose of 10<sup>6</sup> rad at a plane that is 15 m from and perpendicular to the axis of the cylindrical reactor vessel. The shield is thickest along the axis that faces the payload, but it also covers the sides of the reactor to reduce scattered radiation. The two-pi shield utilizes layers of lithium hydride in a honeycomb matrix and tungsten. The second option utilizes an alternative shield configuration consisting of a thin layer of lithium hydride on all exposed surfaces of the reactor and a shadow shield of lithium hydride and tungsten that faces the payload. The shadow shield is selected to provide a prescribed fluence of fast neutrons and gamma dose at a payload dose plane with given diameter and distance from the reactor.”

The ALKSYS code was used to estimate masses of the various subsystems of the vehicle. The lithium cooled UN reactor option was selected to provide mass estimates of the reactor and shield. The shadow shield configuration was selected with the same radiation requirements as imposed for the two-pi option as discussed above.

## Trajectory Simulation

The computer program VARITOP<sup>11,12</sup> was the primary tool used for trajectory analysis in the HOPE study. VARITOP is a low-thrust trajectory optimization program that was developed by the Jet Propulsion Laboratory (JPL) and first used in the 1970's. It is now widely used at JPL, Glenn Research Center, and Marshall Space Flight Center for preliminary mission design studies. It's sister program, SEPTOP, was used to provide trajectory support for the Deep Space 1 mission.

### Heliocentric Analysis Method

VARITOP is used for the heliocentric phase of the trajectory; it is a two-body, Sun-centered analysis tool. The planets are assumed to be massless, and targeting constraints match planetary positions and velocities relative to the Sun. Solution of the problem involves numerical integration of the state and costate or variational equations and the solution of a two-point boundary value problem to satisfy terminal constraints. The optimization, based on the Calculus of Variations, allows users to optimize many design variables. Departure date, flight time, and power required were some of the variables optimized in the HOPE mission analysis.

### Planetocentric Analysis Method

VARITOP also offers several endpoint bias conditions that address the planetary departure and arrival phases of the trajectory. Of these, the most useful for this study is the low-thrust escape or capture spiral bias. For this option, it is assumed that the spacecraft departs from or is captured into a circular orbit around the planet using

the low thrust propulsion system. The formulation of the performance equations for these spiraling escape or capture maneuvers can be found in the paper, “Performance Computations With Pieced Solutions of Planetocentric and Heliocentric Trajectories for Low-Thrust Missions,” by Melbourne and Sauer<sup>13</sup>.

The current version of VARITOP, VARITOP 2000, performs one spiral capture maneuver at the target body; the HOPE mission requires two. The capture maneuver at Jupiter consists of a spiral descent to the mean altitude of Callisto’s orbit around Jupiter, and then another spiral around Callisto to descend to an orbit that is 500 km above the surface. For piloted vehicles, this same problem is encountered upon Callisto orbit departure, where two departure spiral maneuvers are required to escape Jupiter. There are 2 ways to account for the additional  $\Delta V$  needed for the Callisto spiral: A) let VARITOP compute the spiral down to the altitude of Callisto’s orbit around Jupiter, then, outside of VARITOP, calculate the additional  $\Delta V$  needed and account for that additional propellant separately, or B) let VARITOP compute the spiral down to an altitude slightly lower than that of Callisto’s orbit around Jupiter, that altitude is calculated in such a way that the resulting spiral maneuver performs the equivalent  $\Delta V$  of both the Jupiter-centered and Callisto-centered spiral maneuvers. The first method was used for the MPD missions. The fusion-powered missions required a completely different strategy.

For some combinations of vehicle acceleration and spiral initial or final altitude, the VARITOP spiraling approximations are not valid. This was the case for the fusion-powered missions considered. For those three fast missions, the initial vehicle acceleration was between 0.0005-0.0008 g’s, with higher accelerations at subsequent mission phases due to propellant depletion. For these cases, Figure 10 was used to approximate the velocity increment needed to escape from, or capture into, planetocentric orbits for cases where VARITOP could not. This figure was first generated by Sandorff<sup>4</sup>, and is based on the work of Irving<sup>15</sup> and Tsien<sup>16</sup>.

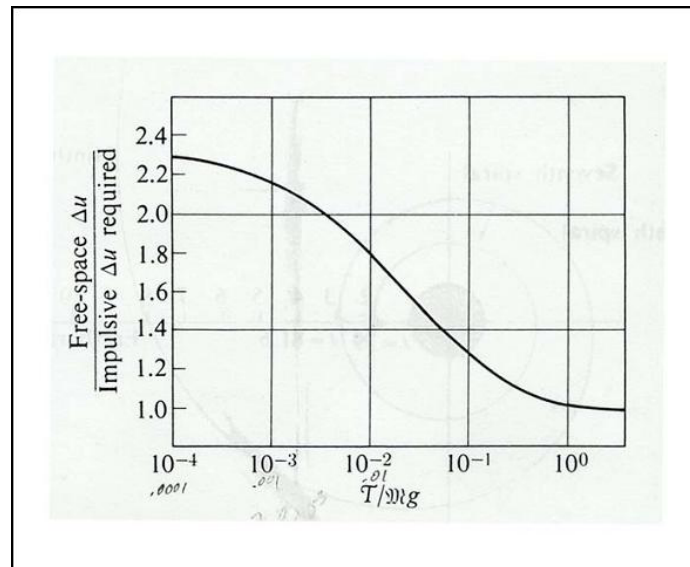
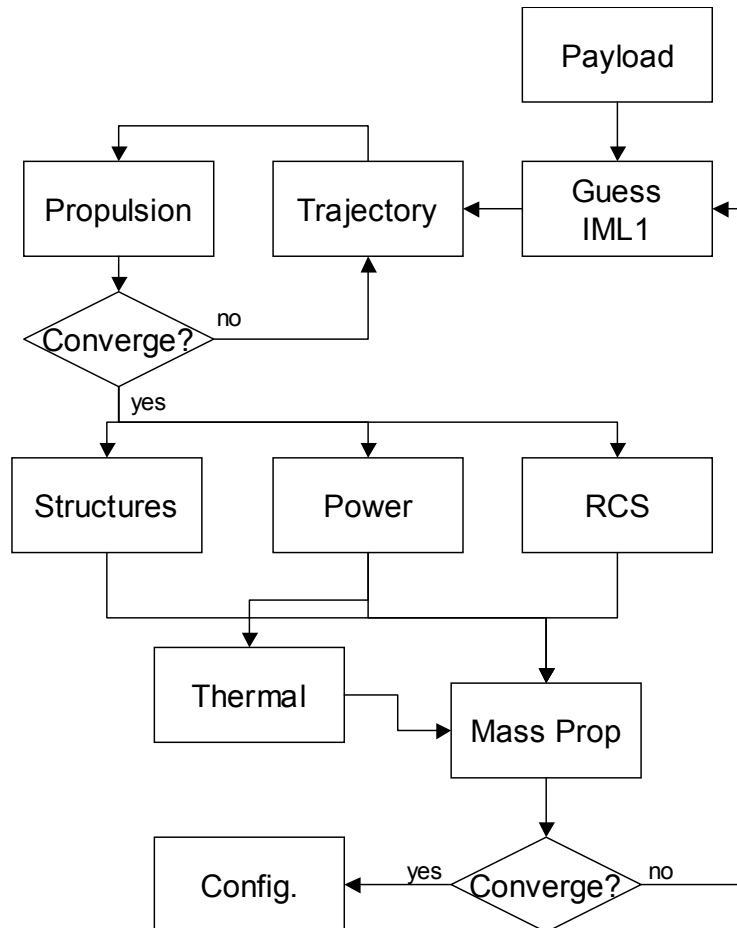


Figure 10 – Penalty for low thrust in escape maneuver from satellite orbit, as compared to impulsive thrust (tangentially directed thrust)<sup>17</sup>

## Vehicle Design

A significant amount of interaction took place between the various disciplines during the design process. Therefore vehicle design becomes an iterative process, with substantial data transfer between the various disciplines. The vehicle design process is illustrated in Figure 11. Engineers at LaRC defined vehicle payloads such as the Transhab, lander, surface habitat and ISRU plant. After a few initial iterations the mass and

envelope volume remained relatively constant. The project lead would next estimate a total mission time and a total initial mass required at L1 (IML1) for the vehicle, using results from previous iterations and total mission times as a guide. The trajectory analyst would take that data and calculate optimal planetocentric and heliocentric trajectories that met the total mission requirement. In calculating these trajectories, the analyst assumed propulsion system performance parameters such as jet power, specific impulse and specific power. These assumed values were passed to the propulsion analyst for verification. The two analysts iterated until convergence on the aforementioned performance parameters was achieved.



**Figure 11 - RASC HOPE design process data flow**

At this point many of the required analyses were performed in parallel. The trajectory analyst also provided the RCS analyst with a timeline of vehicle mass throughout the mission. This ensured that the RCS system could be designed to meet pointing and docking requirements for the mission. The trajectory analyst was also required to provide propellant mass requirements to the structural analyst. The propulsion analyst also outlined major propulsive loads. The structural analyst then determined tank requirements and structural truss masses. The power analyst ensured that the power system was able to start up the propulsion system and also meet other power demands from the payloads and the other subsystems. The thermal analyst received inputs from the propulsion and power systems and from the payloads; these were used to determine radiator areas and masses. The thermal analyst also calculated cryocooler masses and areas based on the tankage requirements obtained from the structural analysis. Finally the mass properties analyst received inputs on all of the subsystems and combined them to produce a resultant IML1 and mass schedule. If these values did not agree with the various assumptions, the project lead assumed another IML1 and another iteration was performed. If the values agreed

within a reasonable error all of the above data was given to the configuration analyst for layout and CAD rendering.

### Trajectory and Configuration Summaries

Each trajectory is optimized to give a maximum payload, subject to a given set of constraints and independent variables. For the fusion-powered missions, the mission time was constrained to 650 days (excluding Earth escape and capture times). This time was selected through a series of compromises. The team wanted to analyze a short mission in order to demonstrate the capabilities of the MTF device, however, maximizing payload mass typically extends the trip time. Another important consideration was the spacecraft's distance from the Sun. Missions of 650 days or less in duration generally maintained a distance of 1 AU or more from the Sun throughout the mission; longer missions came closer to the Sun, resulting in greater radiation exposure for the crew. In an attempt to limit the harmful radiation dose from the Sun, shorten the duration, and maximize payload delivery, a 650-day mission was selected.

While the mission duration was fixed, the flight time for the outbound and return trajectory legs was not. The final optimized missions have return trajectory legs that are shorter than the outbound trajectories. This is to be expected because the vehicle thrust-to-weight ratio on return is much higher than at the start of the mission.

Note that VARITOP is allowed to select the power level and departure date that will optimize the mission performance. The final results for the three fusion-powered vehicles considered are given below.

#### D-D MTF 30-day Stay

**Table 3 - D-D MTF 32-day Stay Summary Information**

		Mission Timeline	
		Time	Mass
		(days)	(mT)
Total Mission Duration ~ 654 days			
Outbound Leg Departs 4/22/2045			
Flight to Callisto ~ 331 days			
Time in Callisto Orbit ~ 33 days	Depart L1 Station	0	650
Total time thrusting ~ 258 days	Thrust off	51	630
Returns without Surface Habitat, ISRU, and Transport (120 mt total)	Thrust on	240	630
Isp = 70,400 sec	Arrive Callisto Orbit	331	595
Jet Power = 1.072 GW	Depart Callisto Orbit	365	475
Propulsion System Specific Mass = 0.022 kg/kW	Thrust off	440	445
Initial Acceleration = 0.0005 g's	Thrust on	614	445
Final Acceleration = 0.0007 g's	Arrive L1 Station	654	430

The HOPE vehicle configuration is designed for launch on a Delta IV type expendable launch vehicle. Multiple launches and in-space assembly will be required due to the overall size and mass of the vehicle. The payload envelope of the launch vehicle is assumed to be approximately 5.0 meters in diameter by 17.0 meters long.

The major components of the MTF baseline vehicle are the six liquid hydrogen (LH2) tanks, the deuterium tank, the reaction control system (RCS) thrusters and propellant tanks, dual two-sided radiators for high temperature, medium temperature, and crew/avionics heat rejection, a SP-100 reactor, four deuterium-tritium tanks, and a water filled tank which provides radiation shielding for the vehicle. A single magnetized target fusion (MTF) engine is located at the aft end of the vehicle. The HOPE vehicle payload consists of a surface habitat module, a Transhab module, a lander, and an ISRU. Structural support of the HOPE vehicle components is provided by open truss segments. The main propellant tank cluster has additional support at the forward and aft ends. The payload modules dock to a single node located at the forward end of the vehicle.



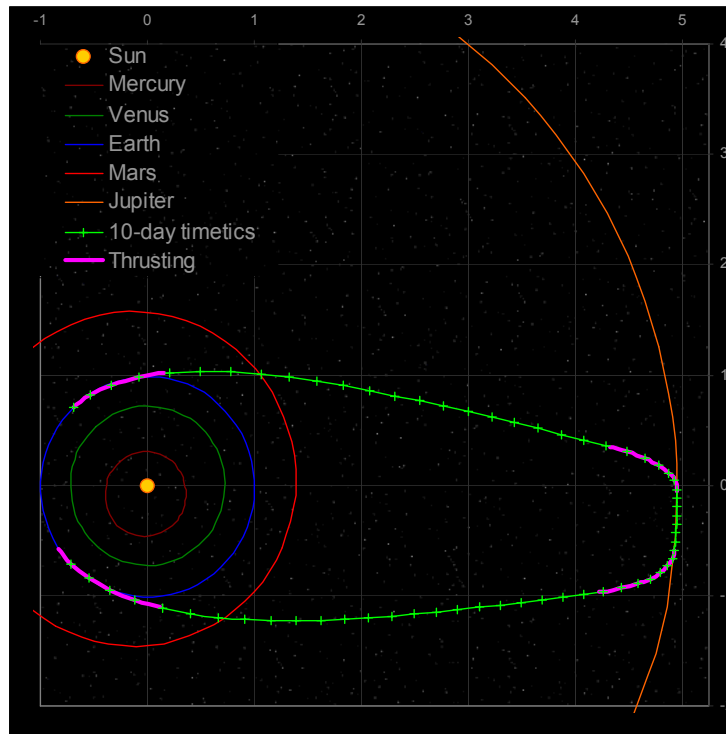


Figure 12 - Trajectory Graph for D-D MTF 30-day Stay Option

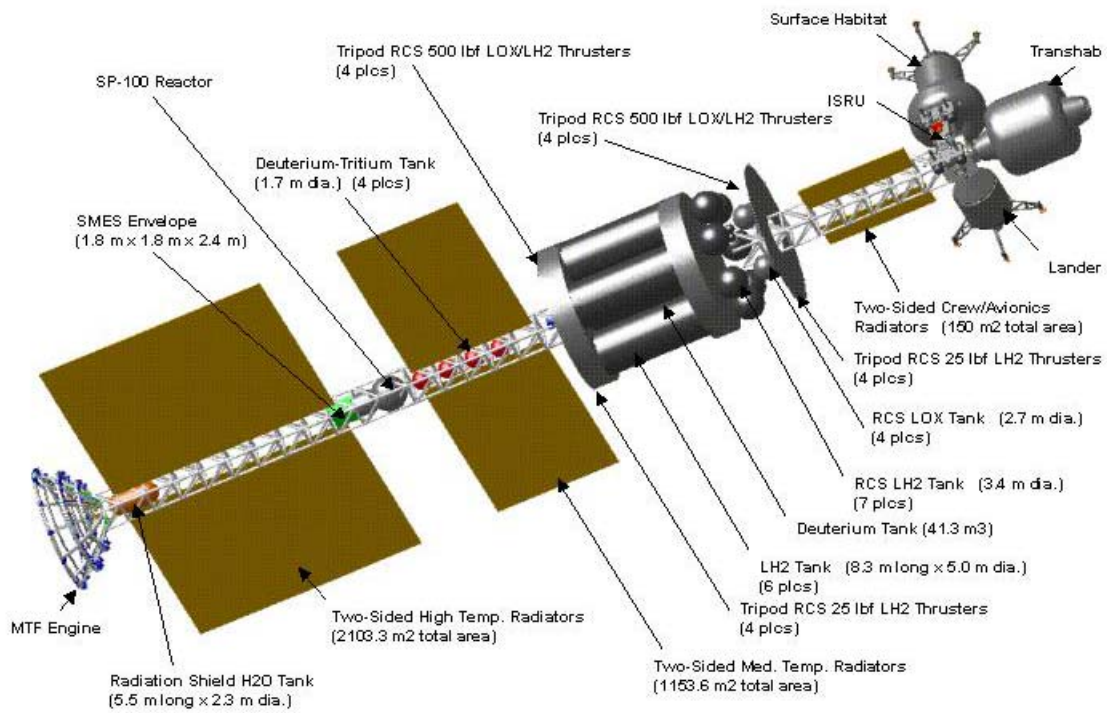
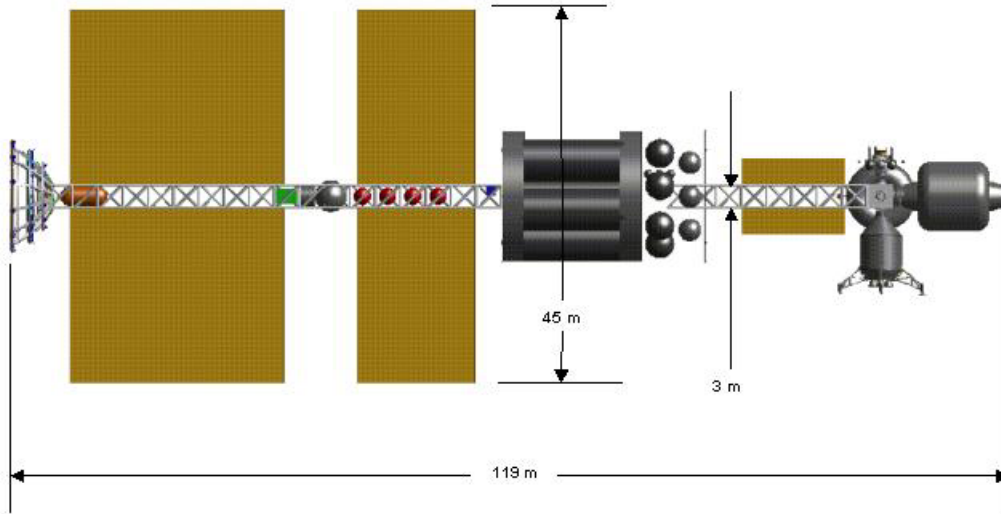
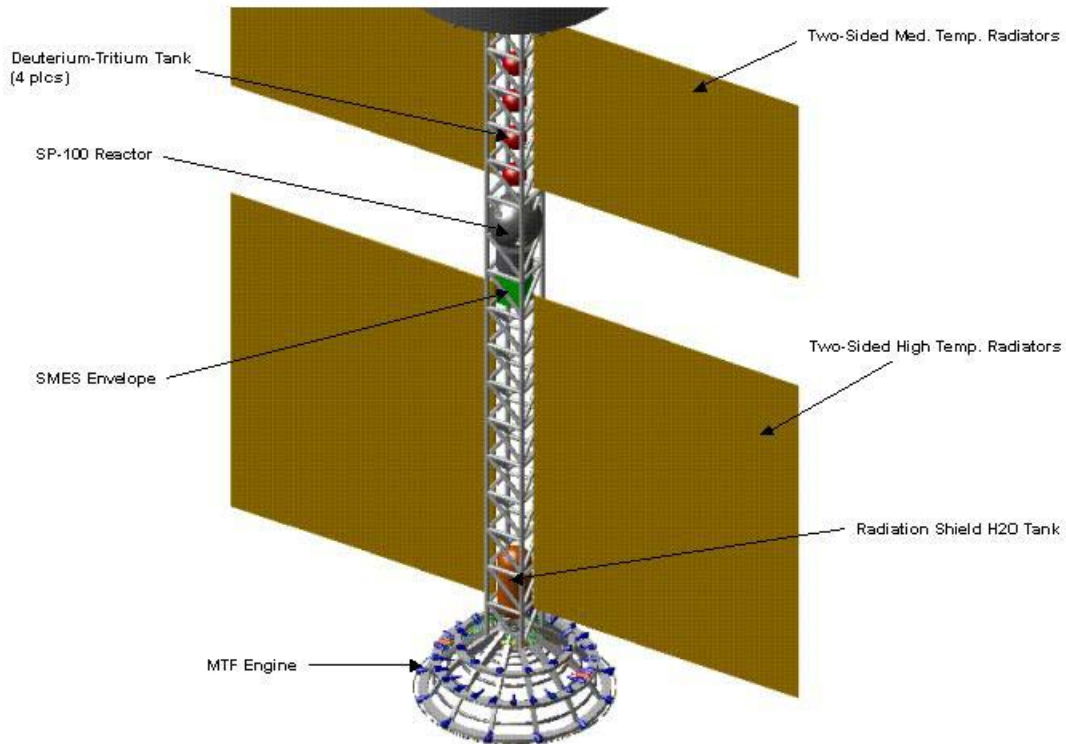


Figure 13 - MTF D-D 30-Day Stay Vehicle

The fully assembled vehicle is approximately the size of a standard football field. The HOPE vehicle overall deployed dimensions are approximately 45 meters in width by 119 meters long.



**Figure 14 - MTF D-D 30-Day Stay Vehicle Overall Dimensions**



**Figure 15 - MTF D-D HOPE Vehicle Aft End Detail**

The HOPE vehicle propulsion system components are located in as close proximity as possible to the MTF to minimize the weight and routing complexity of the required propellant lines, coolant lines, and power system cables.

The RCS is located near to the center of mass of the vehicle. The RCS thrusters are located at a minimum distance from the RCS propellant tanks to minimize the weight and complexity of the associated plumbing required. The crew/avionics radiators are located adjacent to the payload area to minimize the length of the required coolant lines.

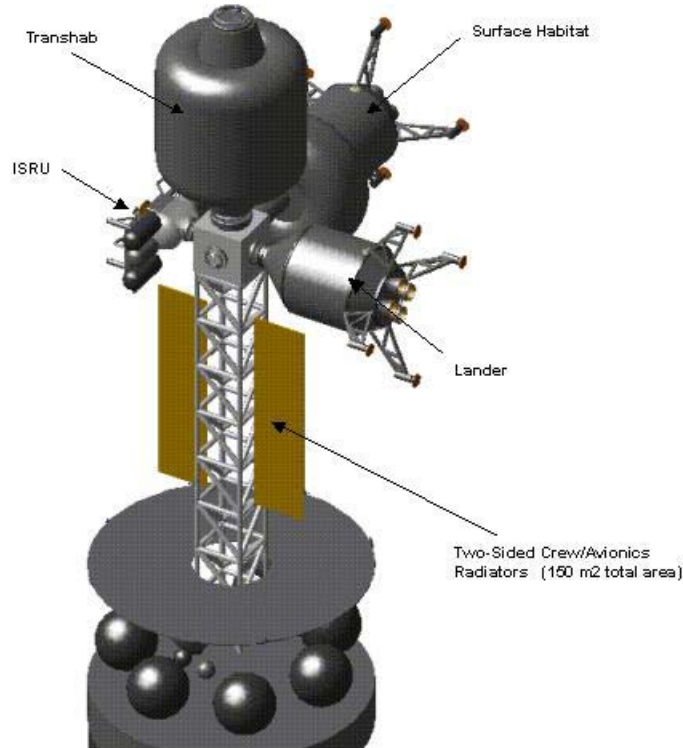


Figure 16 - MTF D-D HOPE Vehicle Forward End Detail

**D-D MTF 180-day Stay**

**Table 4 - D-D MTF 180-day Stay Summary Information**

Total Mission Duration ~ 652 days	Mission Timeline		
Outbound Leg Departs 4/26/2045		Time	Mass
Flight to Callisto ~ 249 days		(days)	(mT)
Time in Callisto Orbit ~ 183 days	Depart L1 Station	0	750
Total time thrusting ~ 212 days	Thrust off	45	717
Returns without Surface Habitat, ISRU, and Transport (120 mt total)	Thrust on	177	717
Isp = 70,400 sec	Arrive Callisto Orbit	249	664
Jet Power = 2.038 GW	Depart Callisto Orbit	432	544
Propulsion System Specific Mass = 0.022 kg/kW	Thrust off	492	499
Initial Acceleration = 0.0008 g's	Thrust on	617	499
Final Acceleration = 0.0013 g's	Arrive L1 Station	652	473

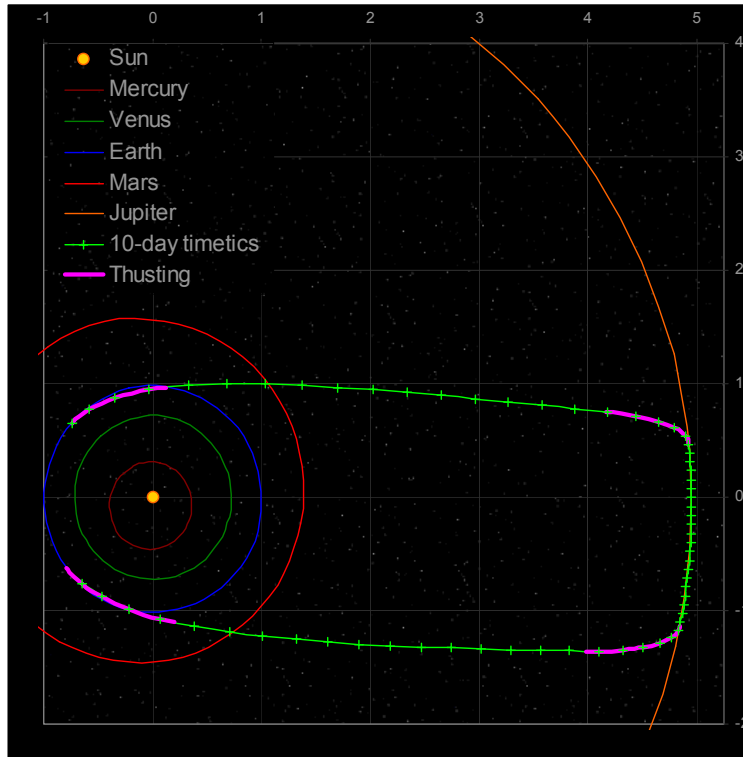


Figure 17 - Trajectory Graph for D-D MTF 180-day Stay Option

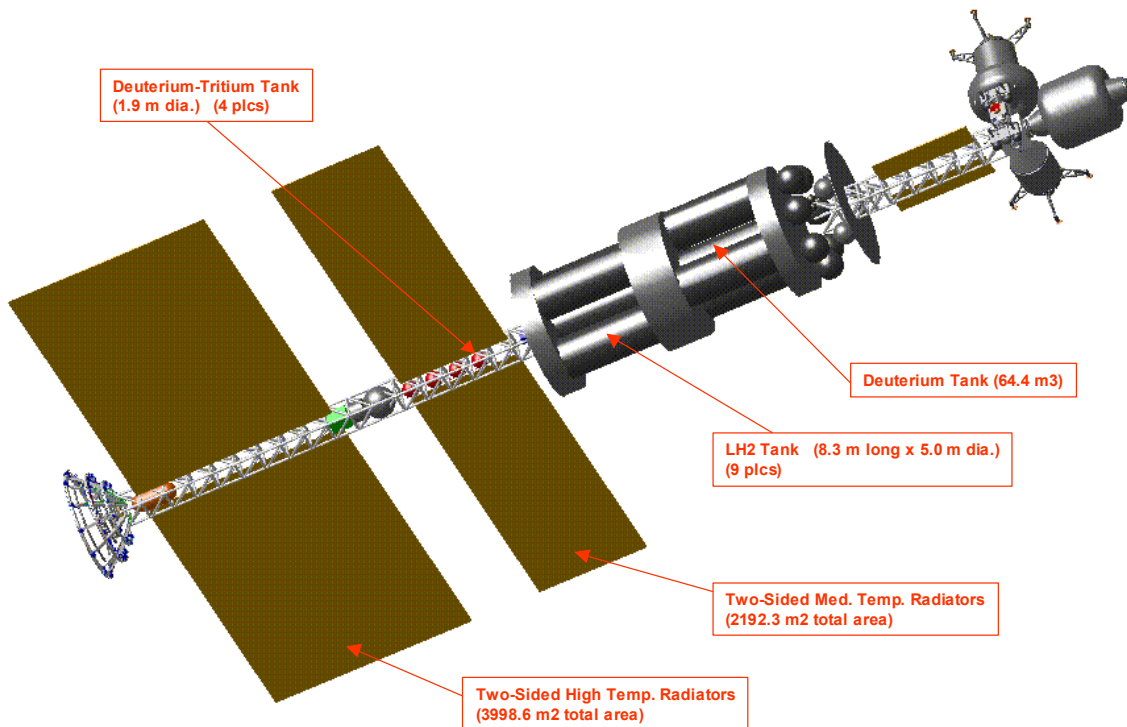


Figure 18 – Vehicle Layout for D-D MTF 180-day Stay Option

The figure above shows the configuration for the 180-day mission. The call-outs on the figure indicate the differences between this configuration and the baseline configuration.

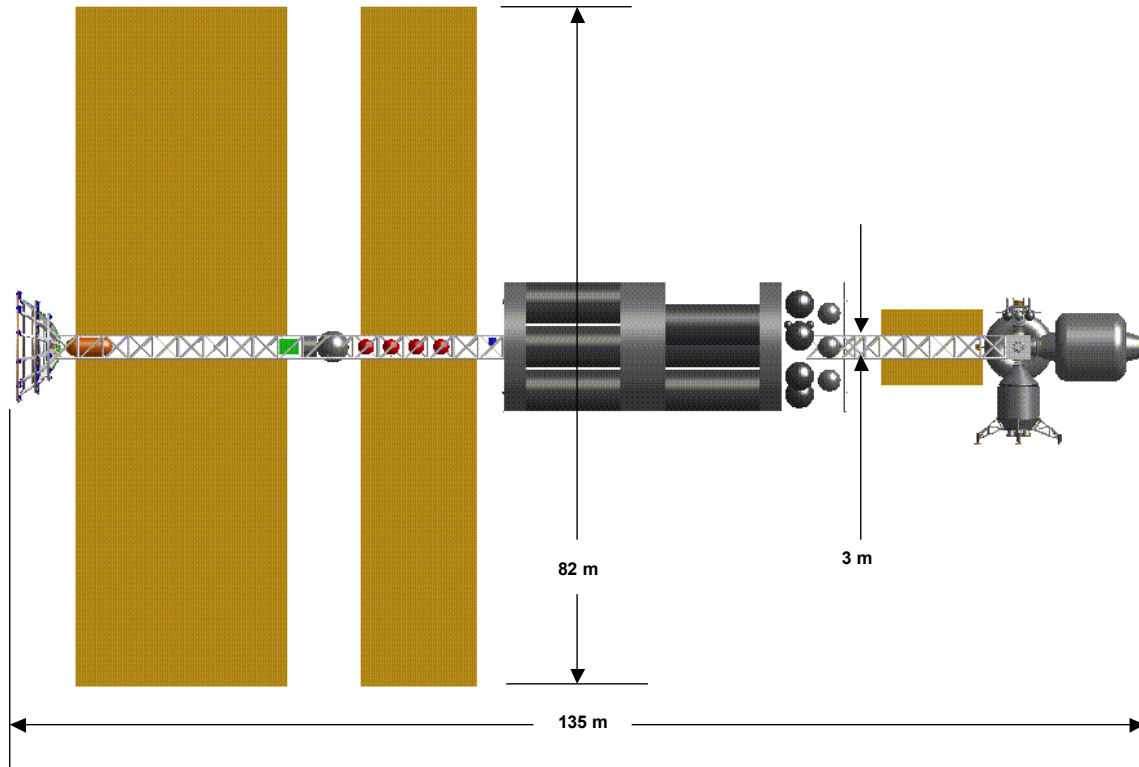


Figure 19 – Vehicle Dimensions for D-D MTF 180-day Stay Option

**D-He<sup>3</sup> MTF 180-day Stay**

**Table 5 - D-He<sup>3</sup> MTF 180-day Stay Summary Information**

Total Mission Duration ~ 652 days	Mission Timeline	
Outbound Leg Departs 4/27/2045	Time	Mass
Flight to Callisto ~ 249 days	(days)	(mT)
Time in Callisto Orbit ~ 183 days	Depart L1 Station	0
Total time thrusting ~ 215 days	Thrust off	46
Returns without Surface Habitat, ISRU, and Transport (120 mt total)	Thrust on	176
Isp = 77,000 sec	Arrive Callisto Orbit	249
Jet Power = 2.071 GW	Depart Callisto Orbit	432
Propulsion System Specific Mass = 0.0193 kg/kW	Thrust off	493
Initial Acceleration = 0.0008 g's	Thrust on	616
Final Acceleration = 0.0013 g's	Arrive L1 Station	652
		445

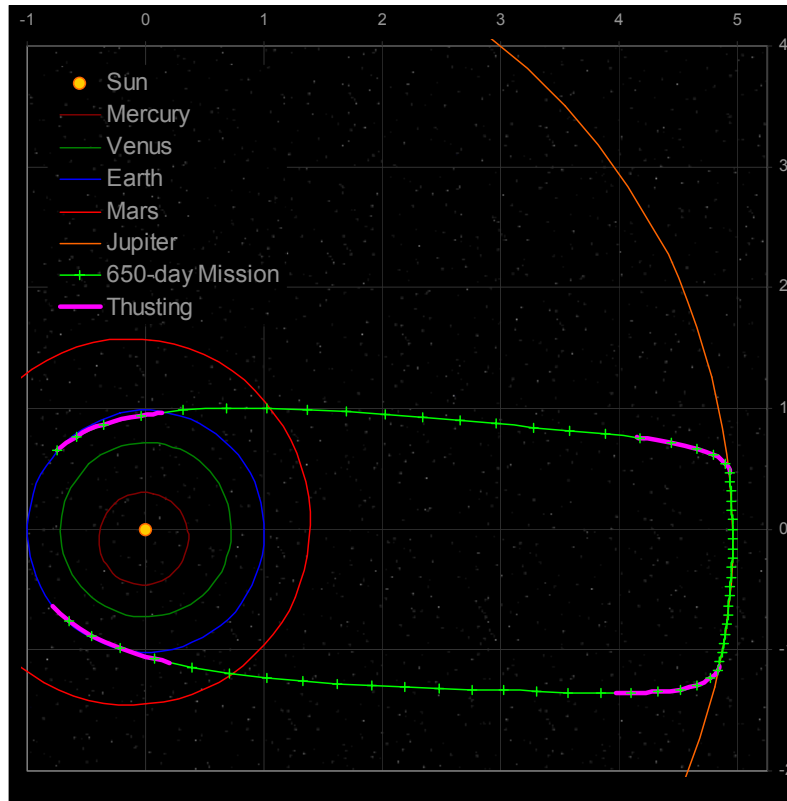


Figure 20 - Trajectory Graph for D-He3 MTF 180-day Stay Option

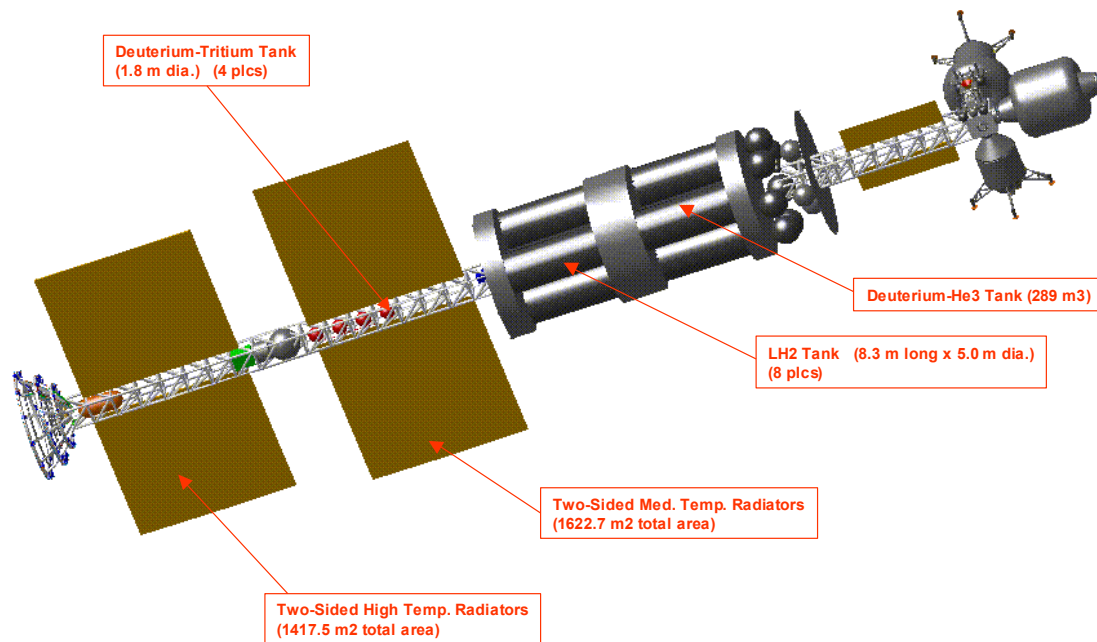
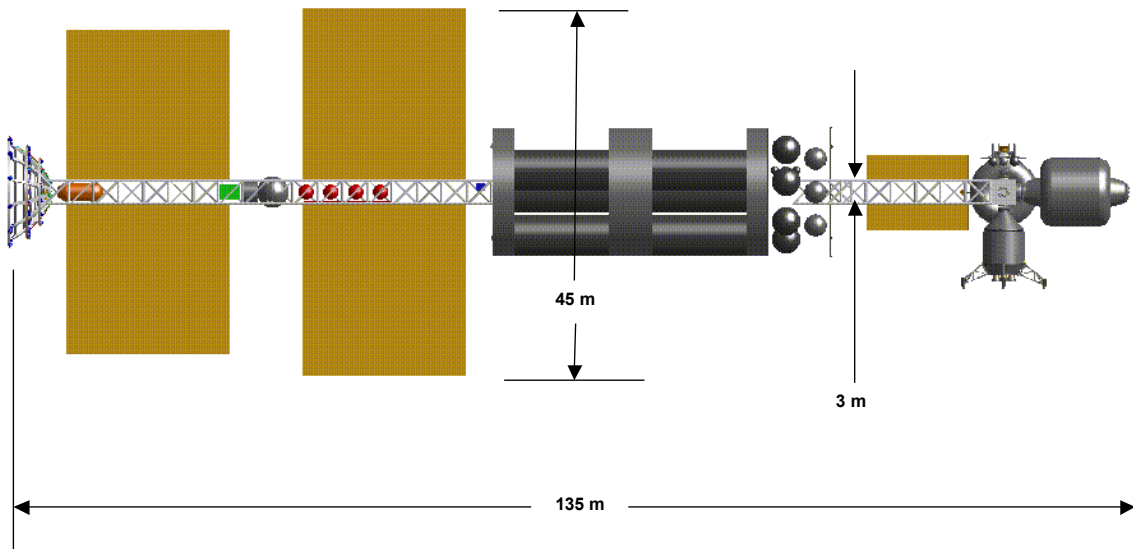


Figure 21 – Vehicle Layout for D-He<sup>3</sup> MTF 180-day Stay Option

This figure shows the configuration of the 180-day mission vehicle that uses D-He3. The callouts show the differences in the vehicle from the baseline configuration.



**Figure 22 – Vehicle Dimensions for D-He<sup>3</sup> MTF 180-day Stay Option**

### MPD Missions

There are two vehicles for each of the MPD missions. Cargo (surface habitat, ISRU, and transport vehicle) is pre-deployed on a separate vehicle from the crew. The trajectory optimization method is the same for both vehicles. The flight time for both vehicles was modeled after the Glenn Research Center team's MPD missions. This was done so that the effects of different technologies between the cases could be analyzed. For these trajectories, VARITOP was able to approximate the Jupiter capture and escape spirals, while the Earth and Callisto capture and escape spirals had to be approximated outside of the program. The Earth spirals, because the altitude at L1 in combination with the thrust-to-weight ratio of the vehicle was outside of the applicability of VARITOP's approximation technique, and Callisto, because VARITOP can only spiral about the destination planet of Jupiter.

### MPD Thrusters

The Magnetoplasmadynamic (MPD) thruster is a member of the electromagnetic class of electric propulsion systems. These thrusters use electromagnetic forces to accelerate plasma propellant to speeds in excess of 50 km/sec. With specific impulse values reaching 5,000 seconds and thrust values up to 2 Newtons, the MPD thruster has a very competitive performance when compared to other electric propulsion systems.

An MPD thruster makes use of coaxially arranged electrodes consisting of a center spike cathode and an outer annular anode. An inert gas such as Xenon flows between the electrodes from a rear injector plate. An electric potential is applied across the electrodes great enough to ionize the gas. Once ionized, the gas becomes electrically conductive and a current flows from the anode through the gas and to the cathode. This current, along with the electrode geometry, produces an induced circular magnetic field between the electrodes. The resulting Lorentz force caused by the electric and magnetic field accelerates the ionized gas (plasma) in a direction perpendicular to both the electric and magnetic fields. It is this force that is responsible for producing thrust.

The arc discharge between the two electrodes produces a large amount of heat that raises the temperature of the thruster. Most of this heat must be removed by a cooling system to protect the materials. Some MPD thrusters are designed to use this heat to produce additional thrust by thermodynamic expansion. Some MPD thrusters are also augmented by including an external magnetic coil wrapped around the thruster. This coil increases the field strength of the induced circular magnetic field in between the electrodes and can improve performance.

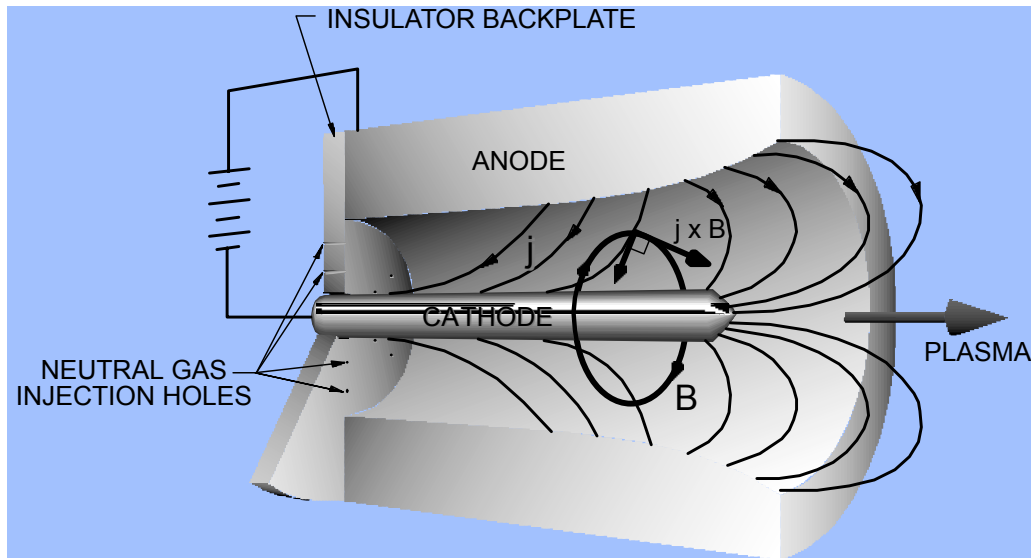


**Figure 23 - Schematic of MPD thruster**

Advances in MPD performance are being pursued by going to higher power systems and using Hydrogen gas as the propellant. Because hydrogen has a light molecular weight, it can exhaust at a higher velocity and result in larger values of specific impulse. It is speculated that specific impulse values as high as 10,000 seconds may be achievable, but this remains to be seen. Although most MPD thrusters tested to date operate at hundreds of Kilowatts, it may be possible to push their power levels as high as Megawatts. The efficiency of these thrusters varies, with between 30% to 50% of the input power being converted into jet power.

The limiting factors of the MPD thruster are based on the plasma physics inside the electrical discharge. For an MPD thruster, most of the losses are associated with the thermal energy created by the high current passing through the plasma. The plasma has an electrical resistance based on the level of ionization that is determined by the voltage across the electrodes. The higher the voltage, the more current passes through the plasma, the stronger the induced magnetic field, and the more thrust produced. Performance is limited by the geometry of the electrodes, the electrical properties of the propellant, and the magnetic Reynolds number.

In order for the propellant to be ionized, a strong enough electric field must be applied. This is essentially a function of the density of the gas, the potential difference across the electrodes, and the distance between the electrodes. These relations govern the mass flow rate, power, and size combinations available to a thruster. The Specific Impulse of the thruster is limited by the magnetic Reynolds number. This is a nondimensional number that represents the ratio of the convective properties of a magnetic field in moving plasma with the ability of a magnetic field to diffuse through the plasma. For plasma moving through a stationary magnetic field, a magnetic Reynolds number less than one indicates that the plasma can move freely through the magnetic field. The limit of this case is when the magnetic Reynolds number equals unity. In this case, the speed of the moving plasma and the rate at which the magnetic field can diffuse through the plasma are equal. If the magnetic Reynolds number becomes greater than unity, the magnetic field is dragged along with the moving plasma and produces a drag force on the plasma flow. This will result in a loss of performance. This may also lead to instabilities within the plasma that can further reduce performance and thruster life.



The life limiting parts of the thruster are the electrodes. The high currents cause sputtering of the electrode material that eventually reduces performance to an unacceptable level. The best erosion rate achievable with current models is 0.5 nanograms per ampere per second or a sputtering of one atom for every  $5E^6$  ions collected on the electrodes. This limits the integrated impulse to approximately  $10^6$  Newton seconds.

### MPD Missions

MPD Mission optimization is similar to that for the fusion missions. The time constraint in this case was modeled after the GRC MPD mission. This was done so that the effects of technology differences between the cases could be assessed. For these trajectories, VARITOP was able to approximate the Jupiter capture and escape spirals, while the Earth and Callisto capture and escape spirals had to be approximated separately (i.e. external to the program). Both the altitude of the L1 point above the Earth and the vehicle thrust-to-weight ratio make VARITOP's approximation technique inappropriate for analysis of the Earth spiral maneuvers. In addition, VARITOP can only model spiral trajectories about the primary attractor in a system; this means that, in the Jovian system, only spiral trajectories about Jupiter – not Callisto – can be modeled. The final results for the two MPD vehicles considered are given below.

### MSR-LMR-MPD

**Table 6 - MSR-LMR-MPD 120-day Stay Summary Information**

<b>Cargo Mission</b>	Mission Timeline	Time (days)	Mass (mT)
Total Mission Duration ~ 1120 days			
Departs 9/2/2041	Depart L1 Station	0	456
Payload Delivered = 120 mT	Thrust off	329	390
Total Power = 11 MW	Thrust on	861	390
Jet Power = 7 MW	Arrive Callisto Orbit	1120	337
Propulsion System Specific Mass = 5.36 kg/kW			
Isp = 8,000 sec			
<b>Piloted Mission</b>			
Total Mission Duration ~ 1661 days	Depart L1 Station	0	1072
Outbound Leg Departs 11/19/2044	Thrust off	34	1049
Flight to Callisto ~ 832 days	Thrust on	60	1049
Time in Callisto Orbit ~ 120 days	Thrust off	284	897
Total time thrusting ~ 812 days	Thrust on	593	897
Returns with 13 mt less consumables	Arrive Callisto Orbit	832	735
Isp = 8,000 sec	Depart Callisto Orbit	952	722
Total Power = 37 MW	Thrust off	1145	591
Jet Power = 24 MW	Thrust on	1540	591
Propulsion System Specific Mass = 5.36 kg/kW	Arrive L1 Station	1661	509
Initial Acceleration = 0.0001 g's			
Final Acceleration = 0.0001 g's			

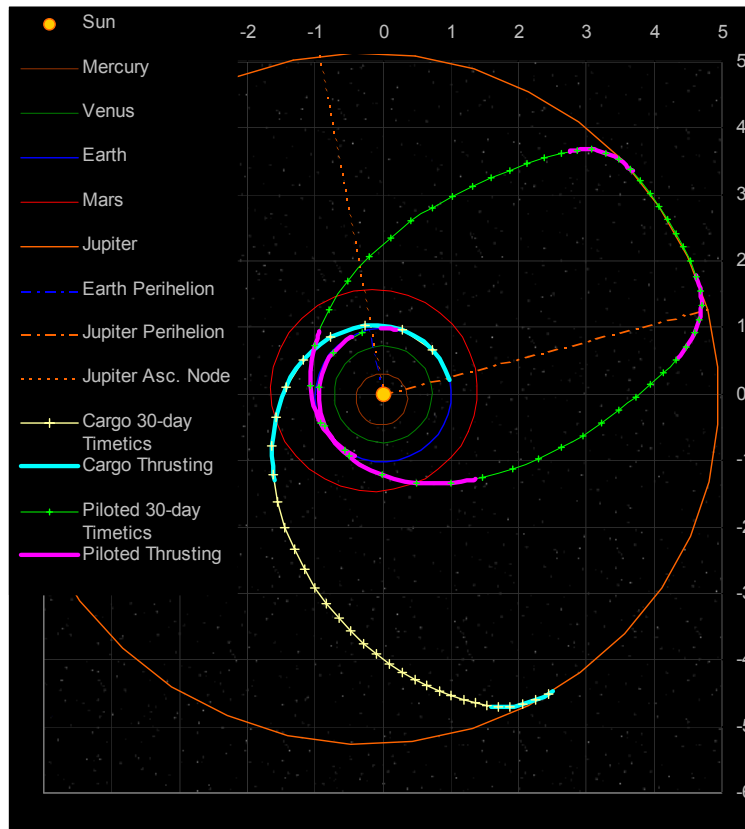


Figure 24 - Trajectory Graph for MSR-LMR-MPD 120-day Stay Option

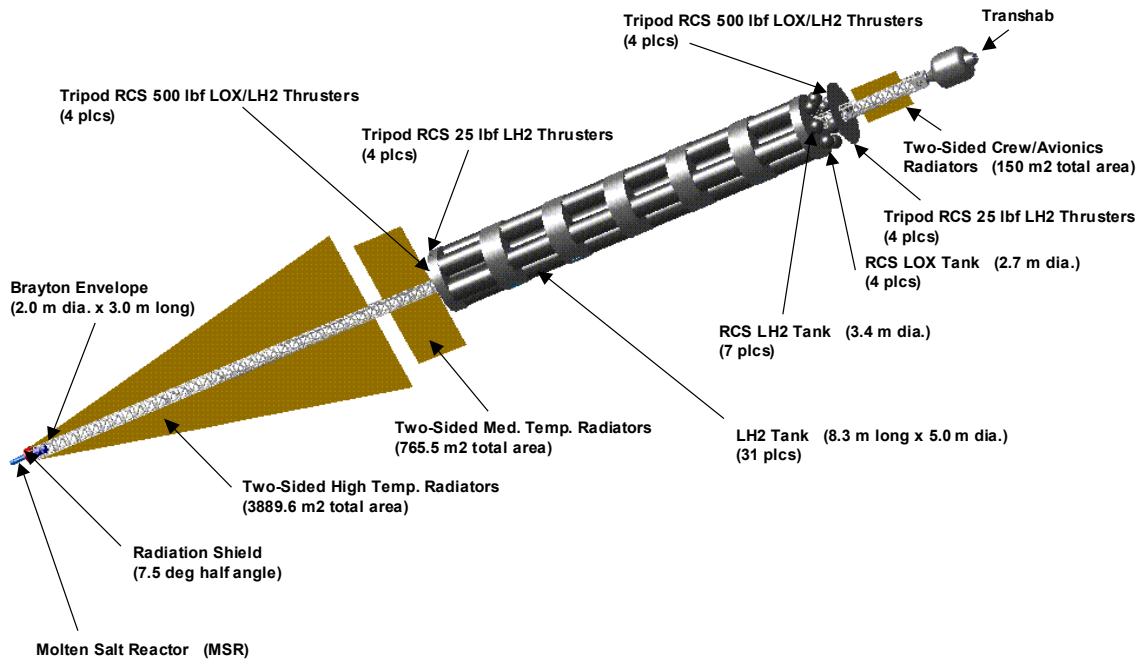


Figure 25 – Piloted Vehicle Layout for MSR-LMR-MPD 120-day Stay Option

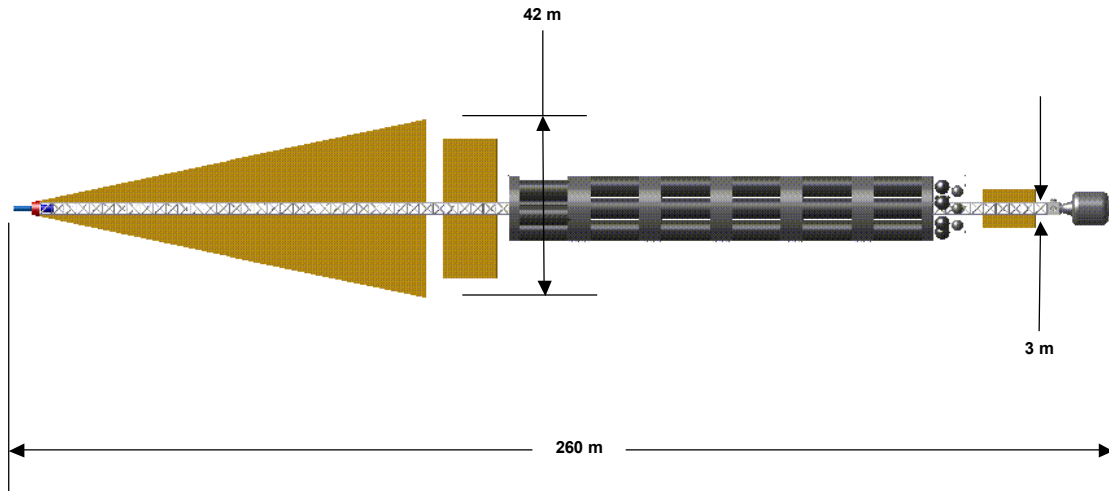


Figure 26 – Piloted Vehicle Dimensions for MSR-LMR-MPD 120-day Stay Option

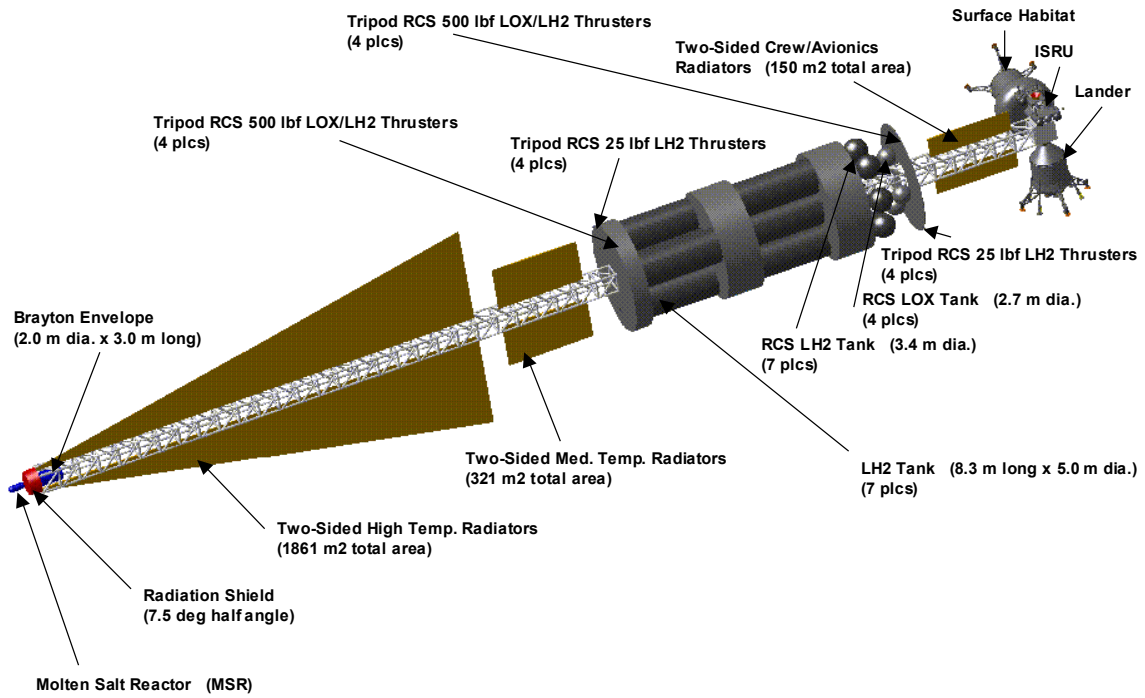
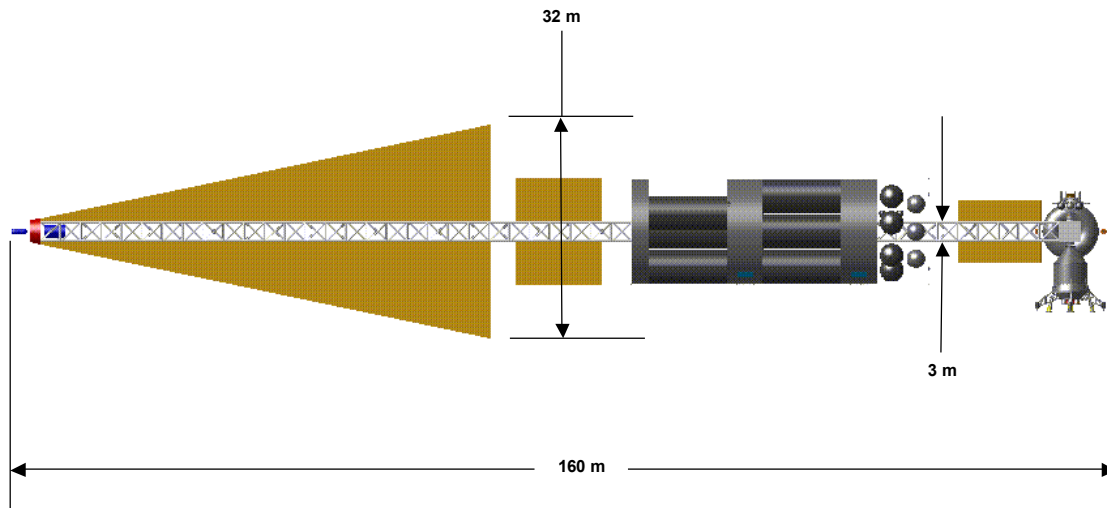


Figure 27 – Cargo Vehicle Layout for MSR-LMR-MPD 120-day Stay Option



**Figure 28 – Cargo Vehicle Dimensions for MSR-LMR-MPD 120-day Stay Option**

Figure 25 and Figure 27 show the MPD propelled concepts which use a liquid metal Rankine reactor to power the systems. The thrusters are very small relative to the vehicle and do not appear in the drawing but are located on the aft facing plate on the structure holding the fuel tanks. The crewed vehicle is 260 m in length and 42 m in width at the widest point on the vehicle. The cargo vehicle is about 160 m in length and about 32 m in width at it widest points.

**SCR-MHD-MPD**

**Table 7 - SCR-MHD-MPD 120-day Stay Summary Information**

<b>Cargo Mission</b>	Mission Timeline	Time (days)	Mass (mT)
Total Mission Duration ~ 1114 days			
Departs 9/10/2041	Depart L1 Station	0	380
Payload Delivered = 120 mT	Thrust off	300	328
Total Power = 10 MW	Thrust on	878	328
Jet Power = 6 MW	Arrive Callisto Orbit	1114	283
Propulsion System Specific Mass = 4.02 kg/kW			
Isp = 8,000 sec			
<b>Piloted Mission</b>			
Total Mission Duration ~ 1658 days	Depart L1 Station	0	882
Outbound Leg Departs 12/06/2044	Thrust off	7	866
Flight to Callisto ~ 833 days	Thrust on	60	866
Time in Callisto Orbit ~ 122 days	Thrust off	253	747
Total time thrusting ~ 693 days	Thrust on	603	747
Returns with 13 mt less consumables	Arrive Callisto Orbit	780	619
Isp = 8,000 sec	Depart Callisto Orbit	955	604
Total Power = 34 MW	Thrust off	1126	498
Jet Power = 22 MW	Thrust on	1548	498
Propulsion System Specific Mass = 4.02 kg/kW	Arrive L1 Station	1658	430
Initial Acceleration = 0.0001 g's			
Final Acceleration = 0.0001 g's			

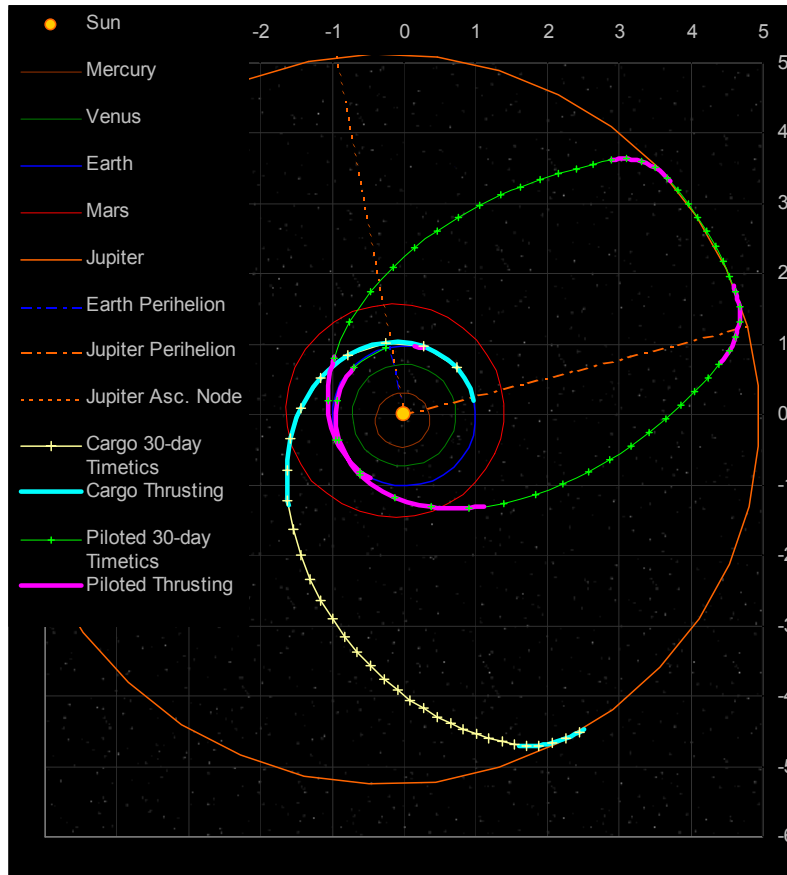


Figure 29 - Trajectory Graph for SCR-MHD-MPD 120-day Stay Option

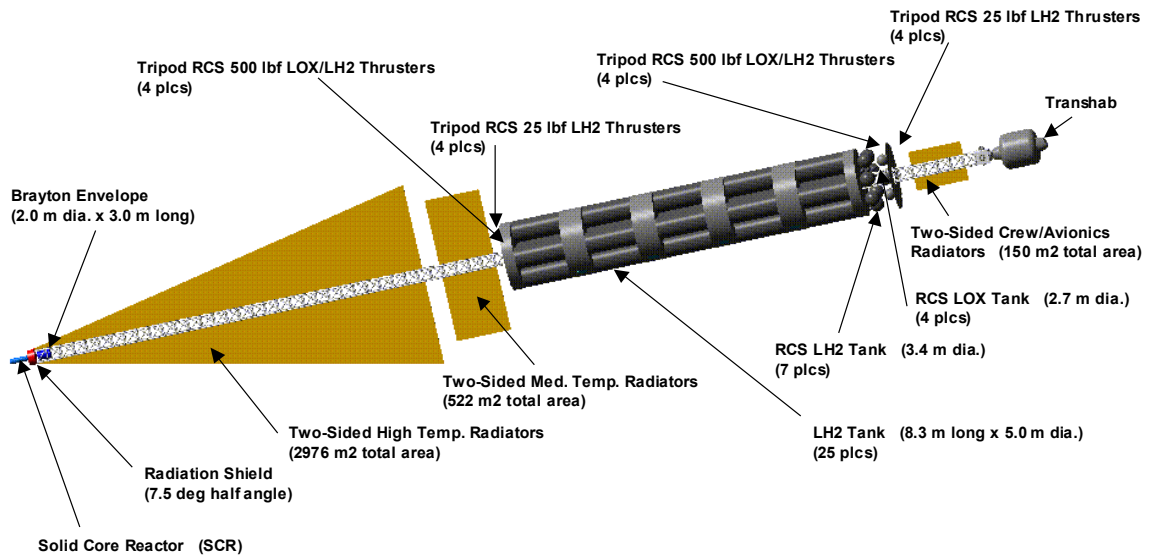


Figure 30 – Piloted Vehicle Layout for SCR-MHD-MPD 120-day Stay Option

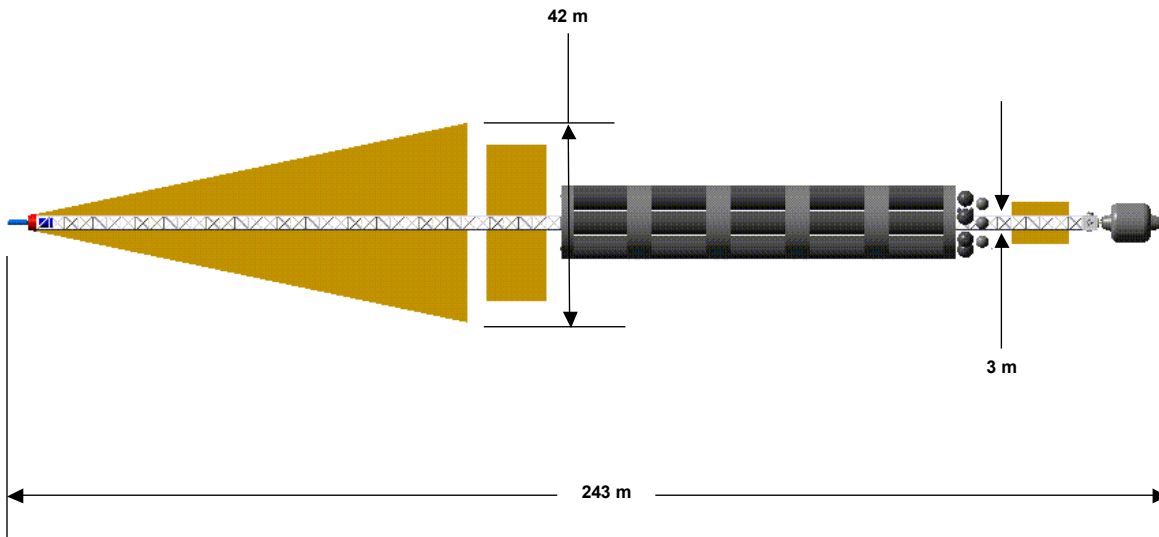


Figure 31 – Piloted Vehicle Dimensions for SCR-MHD-MPD 120-day Stay Option

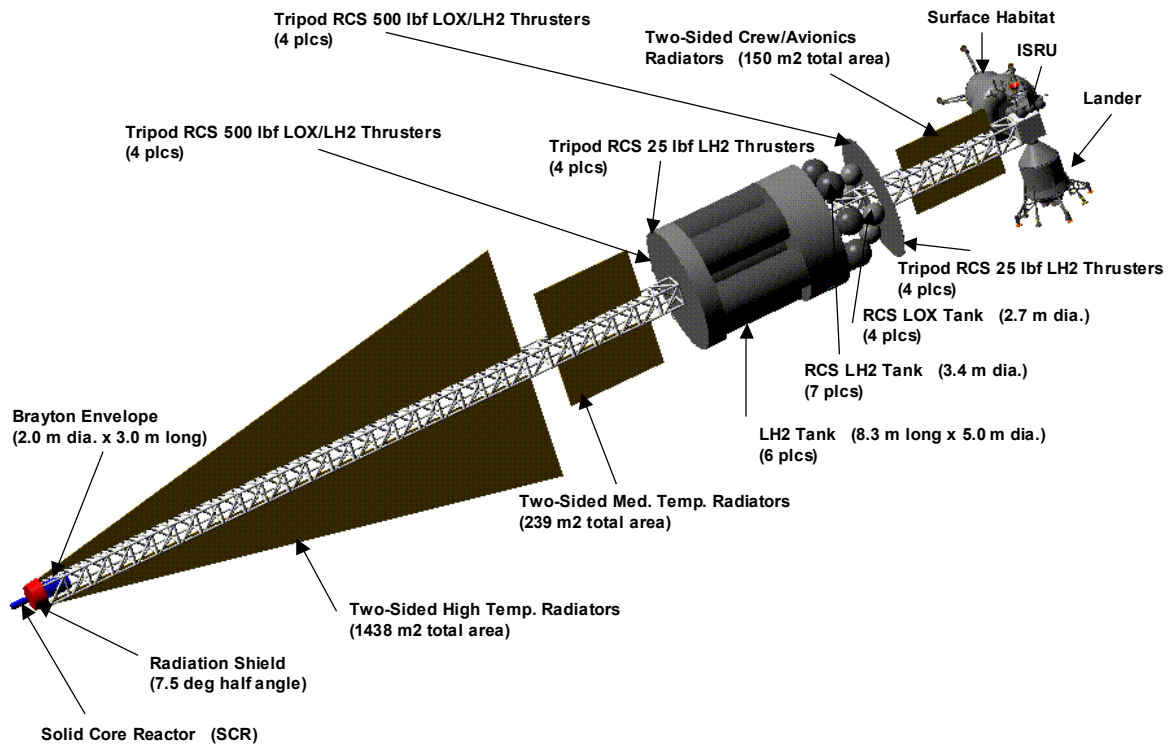
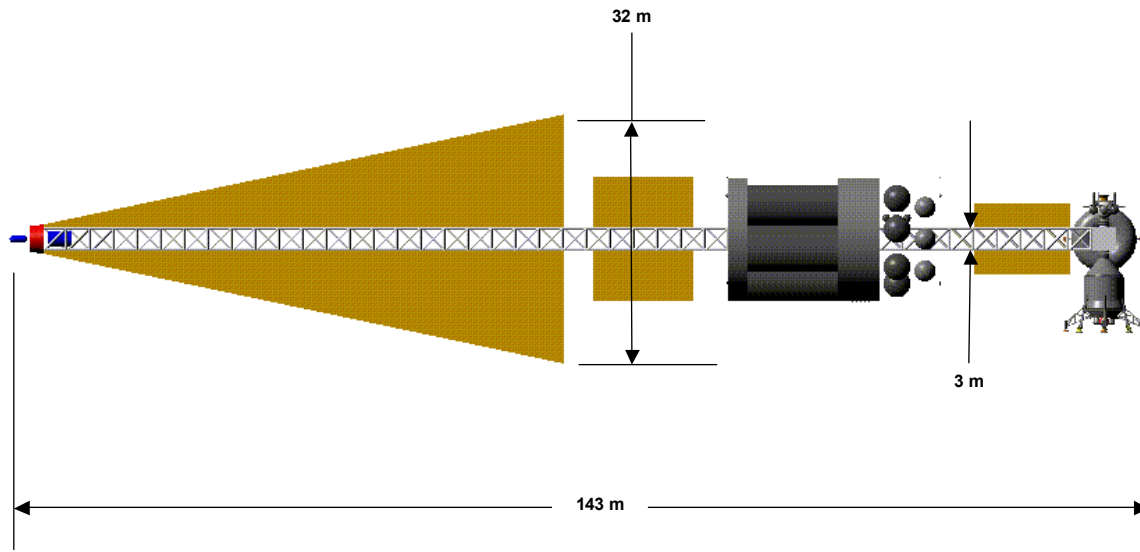


Figure 32 – Cargo Vehicle Layout for SCR-MHD-MPD 120-day Stay Option



**Figure 33 – Cargo Vehicle Dimensions for SCR-MHD-MPD 120-day Stay Option**

Figure 30 and Figure 32 illustrate the solid core reactor, magnetohydrodynamic power conversion option using MPD thrusters. The design is similar to that of the molten salt, liquid metal Rankine option shown above. Again the thrusters are not shown but are mounted on the side of the propellant tank.

### Radiation Exposure

Lower mission times greatly alleviate problems posed by both consumable mass and crew exposure to radiation. Figure 34 illustrates the total exposure expected for the MTF vehicle crew assuming 1 $\frac{3}{4}$  yr mission. The dashed lines indicate the total allowable exposure for a crewmember in low Earth orbit. The letter for each dashed line indicates male or female and the number indicates age. The MTF vehicle would maintain exposure below lifetime limits for males as young as 35 yrs old and females of age 45 or more provided a simple aluminum shield of 4 gm/cm<sup>2</sup> is provided. A somewhat thicker shield, with an areal density of 20 gm/cm<sup>2</sup> of aluminum, will almost permit females of age 35 and above, and males of age 25 and above, to make the journey. Results for several advanced shielding materials are also plotted on the graph.

Calculations of nominal radiation exposure as a function of mission elapsed time were performed by the radiation research group directed by Dr. J. W. Wilson at NASA-Langley. Practically all of the total incurred dose was a result of GCR exposure, and computations were carried out for the various materials (see Figure 34) using the HZETRN heavy ion transport code<sup>18</sup>. The slight increase of slope near the mid-mission time period is due to the added contribution from Jovian trapped electrons for which the transport and incurred dose was computed with the electron code of reference<sup>19</sup>.

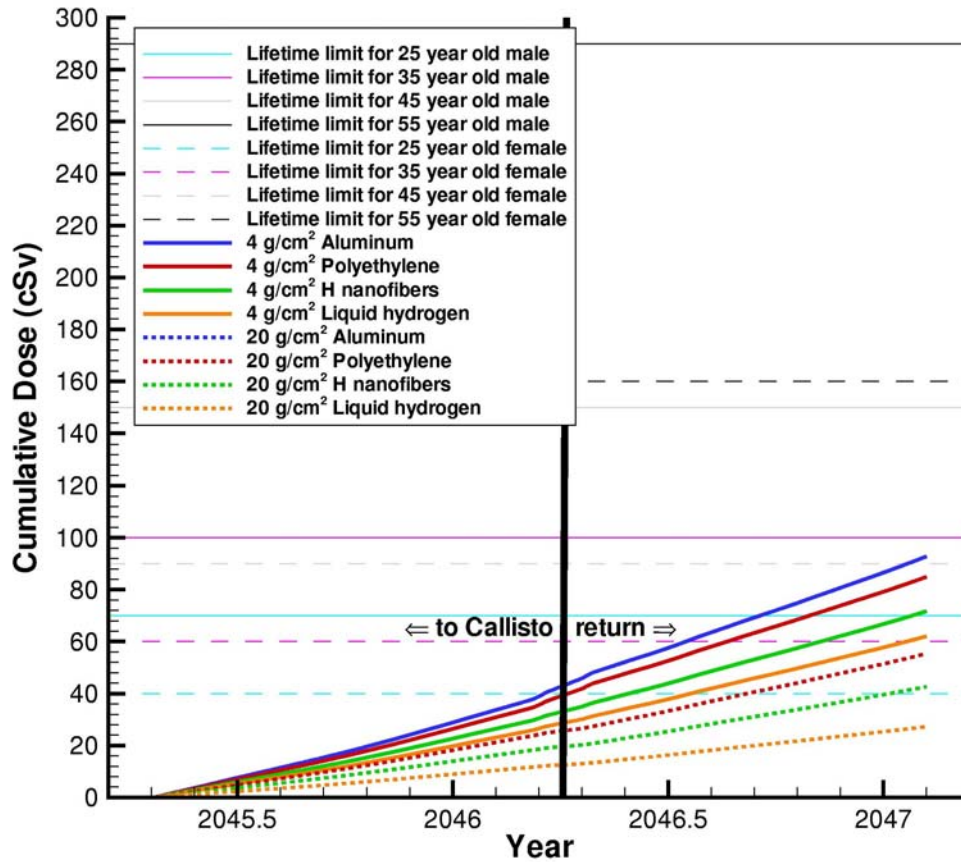


Figure 34 – Cumulative Dose for the MTF 32 day D-D mission to Callisto

### Mass Properties

Table 8 below shows the subsystem mass estimates for each of the concepts analyzed for this study.

Table 8. Vehicle Mass Properties

	<i>MTF D-D 30-day Stay</i>	<i>MTF D-D 180-Day Stay</i>	<i>MTF D- He3 180- Day Stay</i>
Payload	163,933	163,933	163,933
Structural	26,610	34,785	32,060
Reaction Control System (RCS)	12,946	12,989	12,976
Thermal	51,391	76,864	51,306
Power	17,370	17,370	17,370
Main Propulsion	116,021	121,333	118,400
Mass Margin (30%)	116,564	128,265	118,894
<b>Total Dry Mass</b>	<b>505,110</b>	<b>555,814</b>	<b>515,216</b>
Main Propulsion Propellant	106,000	165,000	142,000
RCS Propellant	34,063	35,348	34,674
<b>IML1</b>	<b>645,173</b>	<b>756,162</b>	<b>691,892</b>



	<b>LMR-MPD Piloted</b>	<b>LMR-MPD Cargo</b>	<b>MHD-MPD Piloted</b>	<b>MHD-MPD Cargo</b>
Payload	57,885	120,000	57,483	120,000
Structural	101,955	33,515	85,605	30,790
Reaction Control System (RCS)	12,990	4,741	13,031	12,903
Thermal	49,966	15,180	42,773	13,976
Power	72,149	37,157	89,371	23,601
Main Propulsion	58,596	17,794	13,134	2,627
Mass Margin (30%)	106,145	68,599	90,610	58,893
<b>Total Dry Mass</b>	<b>459,961</b>	<b>297,260</b>	<b>392,643</b>	<b>255,204</b>
Main Propulsion Propellant	577,000	125,000	460,000	98,000
RCS Propellant	35,375	4,322	37,409	5,330
<b>IML1</b>	<b>1,072,336</b>	<b>426,582</b>	<b>890,052</b>	<b>358,354</b>

## Conclusions

Conceptual designs of vehicle systems for human interplanetary systems were successfully completed. The MTF propulsion system with some technological advanced appears to provide increased mission capability, increased payload ratios, and the elimination of the need for split missions. The MPD vehicles have the advantage of using nearer term technology, but require larger vehicles and split crewed and cargo missions. Finally of the MPD missions considered the MHD power vehicle offers the most mass savings due to the removal of the PPU's.

<sup>1</sup> Statham, G., White, Adams, R. B., Thio, Y. C. F., Alexander, R., Fincher, S., Philips, A., Polsgrove, T., *Engineering of the Magnetized Target Fusion Propulsion System*, AIAA 2003-4526.

<sup>2</sup> Adams, R. B., Alexander, R., Chapman, J., Fincher, S., Hopkins, R., Philips, A., Polsgrove, T., Litchford, R., Patton, B., Statham, G., White, S., Thio, Y. C. F., *Conceptual Design of in-Space Vehicles for Human Exploration of the Outer Planets*, NASA-TP, to be published fall 2003.

<sup>3</sup> Williams, Craig H., Dudzinski, Leonard A., Borowski, Stanley K., Juhasz, Albert J., "Realizing "2001: A Space Odyssey": Piloted Spherical Torus Nuclear Fusion Propulsion" 37th AIAA/ASME/SAE/ASEE Joint Propulsion Conference and Exhibit, 8-11 July 2001, Salt Lake City, Utah.

<sup>4</sup> Thio, Y.C.F., Freeze, B., Kirkpatrick, R.C., Landrum, B., Gerrish, H. and Schmidt, G.R., *High-Energy Space Propulsion Based on Magnetized Target Fusion*, AIAA 99-2703, 1999.

<sup>5</sup> Orth, Charles D., UCRL-JC-129237 Rev. 1, April 20, 1998, prepared for the Ninth International Conference on Emerging Nuclear Energy Systems (ICENES '98), Tel-Aviv, Israel, June 28-July 2, 1998.

<sup>6</sup> Krizan, Shawn et al., personal communications.

<sup>7</sup> Launch Vehicle Analysis (LVA) written by Alan Philips of the Marshall Space Flight Center.

<sup>8</sup> Baumeister, E., Rovang, R., Mills, J., Sercel, J., and Frisbee, R., *A Potassium Rankine Multi-megawatt Nuclear Electric Propulsion Concept*, unknown source

<sup>9</sup> Moyers, J.C., and Nichols, J.P., ALKASYS – A Computer Program for Studies of Rankine Cycle Space Nuclear Power Systems, ORNL-TM-10427, September, 1987.

<sup>10</sup> Buden, D.A., et al., *Selection of Power Plant Elements for Future Space Reactor Electric Power Systems*, LANL-7858, Los Alamos Scientific Laboratory, Los Alamos, NM, September, 1979.

<sup>11</sup> Sauer, C.G., "A Users Guide to VARITOP – A General Purpose Low-Thrust Trajectory Optimization Program," Jet Propulsion Laboratory, November 4, 1991.

- 
- <sup>12</sup> Williams, S.N., "An Introduction to the Use of VARITOP – A General Purpose Low-Thrust Trajectory Optimization Program," Jet Propulsion Laboratory, January 24, 1994.
- <sup>13</sup> Melbourne, W.G., and Sauer, C.G., "Performance Computations with Pieced Solutions of Planetocentric and Heliocentric Trajectories for Low-Thrust Missions," Supporting Research and Advanced Development, Space Programs Summary 37-36, Vol. IV, pp 14-19, Jet Propulsion Laboratory, Pasadena, California 1965.
- <sup>14</sup> Sandorff, P.E., "Orbital and Ballistic Flight; An Introduction to Space Technology," M.I.T. Department of Aeronautics and Astronautics, Cambridge, Massachusetts, 1960.
- <sup>15</sup> Irving, J.H., "Lot-Thrust Flight: Variable Exhaust Velocity in Gravitational Fields," Chapter 10 in *Space Technology*, Howard Siefert, ed., New York: Wiley, 1959.
- <sup>16</sup> Tsien, H.S., "Take-off from Satellite Orbit," *Journal of the American Rocket Society* 23, 1953, p. 233-236.
- <sup>17</sup> Hill, P., and Peterson, C., *Mechanics and Thermodynamics of Propulsion*, 2<sup>nd</sup> ed., Chapter 10, p. 506, Reading, Massachusetts: Addison-Wesley Publishing Co., 1992.
- <sup>18</sup> Wilson, J. W.; Badavi, F. F.; Cucinotta, F. A.; Shinn, J. L.; Badhwar, G. D.; Silberberg, R.; Tsao, C. H.; Townsend, L. W.; and Tripathi, R. K.: "HZETRN: Description of a Free-Space Ion and Nucleon Transport and Shielding Computer Program". Nasa Tech. Paper 3495, May 1995
- <sup>19</sup> Nealy, J. E.; Anderson, B. M.; Cucinotta, F. A.; Wilson, J. W.; Katz, R.; and Chang, C. K.: "Transport of Space Environment Electrons: A Simplified Rapid-Analysis Computational Procedure". NASA TP 2002-211448, Mar. 2002